

A MONTE CARLO CALCULATION OF THE
" RESONANCE ESCAPE PROBABILITY OF THORIUM
IN A HOMOGENEOUS REACTOR

by

David L. ^{Quinn} Bushnell
"

Dissertation submitted to the Graduate Faculty
of the Virginia Polytechnic Institute
in candidacy for the degree of

DOCTOR OF PHILOSOPHY

in

Physics

May 1961

Blacksburg, Virginia

TABLE OF CONTENTS

	Page
LIST OF TABLES	4
LIST OF FIGURES	5
CHAPTER 1. INTRODUCTION	6
1.1 The Problem	6
1.2 The Method	9
CHAPTER 2. BACKGROUND AND LITERATURE REVIEW	13
CHAPTER 3. THE MONTE CARLO MODEL	17
3.1 Outline of the Model	17
3.2 Beginning a Neutron History	24
3.3 The Mean Free Path	25
3.4 The Collision	27
3.5 Tracking the Position	30
CHAPTER 4. NEUTRON-NUCLEUS CROSS SECTIONS	34
CHAPTER 5. COMPUTATIONS AND RESULTS	40
5.1 Resonance Escape	40
5.2 Collision Probabilities	45
CHAPTER 6. ERROR ANALYSIS AND CONCLUSIONS	47
6.1 Monte Carlo Statistics	47
6.2 Probable Error for the Slope of Equation (5.9)	49
6.3 Built in Systematic Errors	51
6.4 Discussion of the Results	52

	Page
6.5 Comparison to Analytical Calculations	54
6.6 Conclusions	62
CHAPTER 7. SUGGESTED EXTENSIONS	64
ACKNOWLEDGMENTS	66
BIBLIOGRAPHY	67
Literature Cited	67
Literature Examined	70
VITA	72
APPENDIX I	73
APPENDIX II	75
APPENDIX III	91
APPENDIX IV	92

LIST OF TABLES

Table		Page
1	Nuclide Number Densities and Cross Sections for Five Concentrations of $\text{Th}(\text{NO}_3)_4$ in Water . .	25b
2	Resonance Parameters	25c
3	Energy Interval Assignments	25d
4	Data From Output Cards	42a
5	Probability Results	42b
6	Comparison of Leakage and Absorption	44a
7	Nuclide Population Control of NoH	44a
8	Results Including Monte Carlo Statistical Probable Error	48a
9	Quantities for Slope Probable Error	50a
10	Sample Data and Results for an Analytical Calculation with $n_{\text{Th}} = .9013 \times 10^{21} \text{atoms/cm}^3$. .	57a
11	Comparison of Monte Carlo and Analytical Values for REP'	61a
12	Effective Resonance Integrals	61b

LIST OF FIGURES

Figure		Page
1	Monte Carlo Flow Diagram for Thorium Resonance Escape	17a
2	Average Source Energy per Slab Versus Z	25a
3	Center of Mass Collision Cone	27a
4	Post Collision Neutron Velocities	27a
5	Tracking Coordinates	30a
6	Thorium Resonance Peaks, 1 and 2	37a
7	Thorium Resonance Peak 4	37b
8	Cross Sections in the Unresolved Region	37c
9	Schematic Illustration of Resonance Escape Probabilities	41a
10	Resonance Escape Probability as a Function of Thorium Number Density	43a
11	Atomic Collision Frequencies	45a
12	Density at 20°C. of $\text{Th}(\text{NO}_3)_4$ Aqueous Solution as a Function of Concentration	46a
13	Probability for an Absorption Given a Thorium Collision	52a
14	Pictorial Concept of Narrow Resonance	54a
15	Position Vectors	54a

CHAPTER 1.
INTRODUCTION

1.1 The Problem

It is the intent of this investigation to prepare a statistical model as an analog to a physical process by employing a random sampling technique which has come to be known as the Monte Carlo method. The physical process is the slowing down of neutrons by collisions with atomic nuclei where one type of nucleus can absorb. A parameter of absorptive moderating systems known as the resonance escape probability (REP) is of interest to reactor physicists and can be estimated from data produced by the statistical model.

The physical system to be considered consists of $\text{Th}(\text{NO}_3)_4$ dissolved in water to provide a finite homogeneous water moderated reactor in the form of a rectangular parallelepiped. A neutron source is produced at the center of one face by a beam of deuterons striking a deuteron target. The neutrons so produced have an energy of about 2.9 Mev. A tritium target can also be used producing neutrons of about 14 Mev. The (d,t) reaction provides larger neutron fluxes than the (d,d) reaction making possible better counting statistics for experiments.

The neutron cross section of a thorium nucleus manifests several resonances and varies rather rapidly with neutron energy for energies between 10 ev. and 1000 ev. The resonance escape probability is a measure of the ability of a neutron to escape being absorbed while its energy is degraded by the moderation process to an energy below 10 ev.

A system, such as the one considered here, which has many types of nuclides present, some of which can absorb neutrons, is too complicated to solve analytically. From an asymptotic approximation for the slowing down density, $q(E)$, an expression for the resonance escape probability can be written in the form

$$p(E) = e^{-\frac{n_{Th}}{\sum_s}} \int_E^{E_0} \frac{\sigma_s \sum_a(E') dE'}{\bar{J}(E') \sum_t(E') E'} \quad (1.1)$$

where $\sum_a(E')$ = the macroscopic absorption cross section at E' .

$\sum_t(E')$ = the total macroscopic cross section at E' .

$\bar{J}(E')$ = an average logarithmic energy decrement for a mixture of nuclides.

σ_s = total scattering cross section for all the nuclides.

E_0 = the source energy.

n_{Th} = the number of thorium atoms per unit volume.

Equation (1.1) is well discussed by Meghreblian and Holmes (12) along with versions for simpler systems. They define

$$p(E) = \frac{q(E)}{q(E_0)}$$

whence (1.1) results for

$$\bar{p} = \frac{\sum_i \xi_i \Sigma_{si}}{\sum_i \Sigma_{si}}$$

$$\xi_i = 1 + \frac{\alpha_i \ln \alpha_i}{1 - \alpha_i}$$

$$\alpha_i = \left(\frac{A_i - 1}{A_i + 1} \right)^2$$

A_i = the atomic mass number of the i^{th} target atom.

It is more convenient for our purposes to use a slightly different definition for $p(E)$. We will define $p(E)$ to be the ratio of the number of neutrons that reach energy E (which is in our case 10 ev.) from the resonance energy region to the number that enter that region from above 1000 ev. The resonance escape formulas are discussed more completely in section 5.1 and reference (12).

1.2 The Method

The Monte Carlo procedure when applied to physical phenomena becomes essentially a "theoretical experiment" in the sense that a hypothetical set of physical occurrences are imagined whose outcomes are decided deterministically or probabilistically from fairly well established physical theories. The "experiment" comes from allowing a series of many events to occur. The theoretical aspect comes from the use of physical theories to provide the distributions for the sampling procedures. The events considered in this paper are collisions between neutrons and atoms of the reactor system. In all such events the energy of the neutron relative to the atoms is high enough so that molecular collisions do not occur and hence a neutron interacts only with member nuclei separately.

The fundamental theorem of the Monte Carlo method for a continuous variable is as follows:

Let $f(x)$ be a real, positive, single valued, continuous function of the variable x defined on the interval $-\infty < x < \infty$ such that

$$\int_{-\infty}^{\infty} f(x) dx = 1.$$

If N_r is a random variable uniformly distributed on

the interval $0 \leq N_r \leq 1$, then the equation

$$N_r = \int_{-\infty}^{X_n} f(x)dx \quad (1.2)$$

implies that X_n is a random variable with frequency function⁽¹⁾ $f(X_n)$.

A proof of this theorem appears in appendix I.

For the discrete case, where there are n mutually exclusive events available one of which is denoted by E_i with probability p_i , we say that event E_m occurs if for a selection of N_r we have

$$\sum_{i=1}^{m-1} p_i \leq N_r < \sum_{i=1}^m p_i \quad (1.3)$$

where N_r is again a random number uniformly distributed on the interval $0 \leq N_r \leq 1$ and $\sum_{i=1}^n p_i = 1$. References (2), (9) and (10) provide good discussions of the Monte Carlo method and its applications.

It is not always easy to invert the integral in equation (1.2) so various tricks have been employed to

(1) Frequency function is often referred to as probability density function (9).

avoid excessive labor. One such trick is known as the rejection technique and is discussed by Kahn (9).

To apply equation (1.3) one subdivides the interval 0 to 1 into subintervals whose lengths correspond to the p_i of the events E_i . When a selection of N_r provides a value that lies in the m^{th} subinterval, equation (1.3) is satisfied and we say that event E_m occurs.

Large capacity high speed computers are needed in order to handle most Monte Carlo problems. The Virginia Polytechnic Institute has an IBM-650 on which we programmed the Monte Carlo model for the thorium resonance escape probability.

Our chief objective is to develop a Monte Carlo model which will provide a better description of the effect of resonance phenomena on the behavior of reactor systems than has been heretofore possible by analytical methods. It is conceded that the Monte Carlo approach is inefficient when compared to analytical methods but where the latter fails we turn to the former as a last resort. Analytical treatments of diffusion and transport phenomena are limited to special cases since there is a lack of knowledge about the transformation kernels appearing in the integral equations.

While waiting for development of the analytical methods it becomes necessary to turn to approximation and sampling procedures. Knowledge obtained in such a manner may lead to advances in the analytical techniques.

CHAPTER 2.

BACKGROUND AND LITERATURE REVIEW

Monte Carlo investigations of resonance escape probabilities have been done by several groups, who have concentrated on heterogeneous systems containing uranium as the resonance absorber. R. D. Richtmyer and collaborators (15), (16) developed a model for a heterogeneous symmetrical array of cylindrical U^{238} fuel rods contained in a water moderator.

As will be the case in this paper, Richtmyer considers neutron-nucleus scattering collisions, absorbing collisions and rectilinear motion between collisions as the possible events for description. Proceeding from the last neutron collision, Richtmyer determines the distance to the next collision by applying the expression

$$l(E) = -\lambda(E) \ln N_r$$

where $\lambda(E)$ = the mean free path at energy E
 $l(E)$ = the distance from the last collision to the next at energy E
 N_r = a random number distributed uniformly on $(0,1]$ and selected by a standard random number algorithm in the computer.

The mean free path $\lambda(E)$ is determined from a knowledge of the total cross section by the relation

$$\lambda(E) = \frac{1}{\Sigma_t(E)}$$

where $\Sigma_t(E)$ = the total macroscopic cross section at energy E.

His first published resonance escape calculation in 1956 (15) employed the Doppler broadening function $\psi(x,t)$ for the uranium cross sections while in a later version in collaboration with Van Norton and Wolfe (16) he included a second Doppler broadening function which describes an interference effect in the cross section. See chapter 5 for definitions and discussions of these functions.

The Richtmyer code was written for an IBM-704 which has considerably more speed and storage than the IBM-650 for which our Monte Carlo was written. He, therefore, has been able to develop a rather flexible program to include some variation in geometry and composition of the reactor. His program employs a hexagonal unit cell parallel to the fuel rods.

Many investigations have been made of the resonance integral $\int \frac{\sigma(E)dE}{E}$ and the effective resonance integral

$$\int_E^{E_0} \frac{\sigma_a \sum_s(E') dE'}{\sum_t(E') E'} \quad (2.1)$$

whose forms should be modified to include Doppler - broadening. A comparison between these investigations and the present one is difficult but possible provided we can accept the conditions concerning the resonance structure necessary for equation (1.1) to be valid. The origin of equation (1.1) and the conditions for validity are given in appendix IV. Dresner (6) has made some of the most extensive investigations of the resonance integral, and calculations based on his work are presented in section 6.5.

Safanov (of the Rand Corporation) (19) has made an investigation of resonance escape probabilities for water-natural uranium homogeneous mixtures with varying amounts of light and heavy water. The calculations for these systems are based on the Boltzmann equation with the diffusion approximation. A multi-energy group solution was carried out using 53 energies selected from the numerous noncoincident resonances of U^{235} and U^{238} . The IBM-701 provided solutions of the 53 simultaneous equations. The energy range 1 ev. to 1000 ev. is used as the resonance range and this interval required 42 of the groups. The

resonances were fit with histograms with only one block to a peak rather than a many block histogram or a Breit-Wigner expression. The definition of the resonance escape probability used by Safanov is the fraction of those neutrons living to energies less than 1000 ev. that survive to energies less than 1 ev. This is essentially the same definition that we use except our lower energy limit is 10 ev. Figure 3 of Safanov's paper displays the resonance escape probability as a function of the ratio of the number of moles of water to the number of moles of uranium. Our Monte Carlo with modifications to handle uranium cross sections should be able to reproduce the topmost curve of that figure if the two methods are compatible.

CHAPTER 3.

THE MONTE CARLO MODEL

3.1 Outline of the Model

Referring to the flow diagram exhibited in figure 1 we see that a neutron history begins by a reading of the source parameters into the machine storage. The energy is placed in a reference location and count boxes are set to zero. The sines and cosines of the velocity direction angles are computed and stored for future reference. The energy dependent mean free path $\lambda(E)$ is determined by the method outlined in section 3.3. The distance to the next (or first) collision is determined as follows:

The probability of a collision in dx at x , where x is the distance along a straight line, is given by

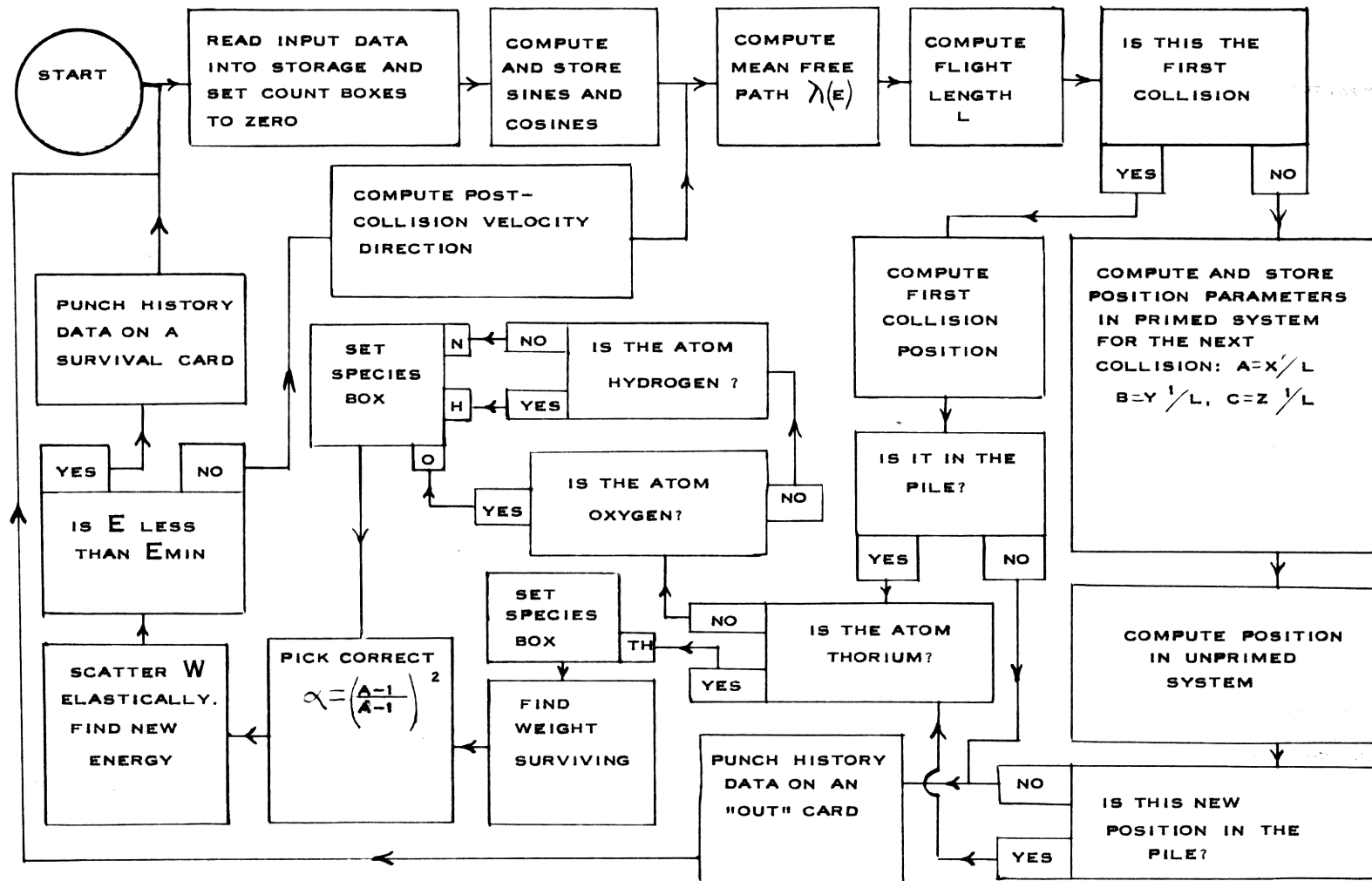
$$f(x)dx = \sum e^{-\Sigma x} dx$$

where $\int_0^{\infty} f(x)dx = \int_0^{\infty} \sum e^{-\Sigma x} dx = 1$

and $f(x)$ = the probability density function (p.d.f.) for x .

We imagine another non-discrete random variable y that has a p.d.f. $g(y)$ such that

$$g(y)dy = f(x)dx \quad \text{where } g(y) = 1.$$



MONTE CARLO FLOW DIAGRAM FOR THORIUM RESONANCE ESCAPE PROBABILITY

FIG. - 1

We then say that the new variable is uniformly distributed and that

$$\int_0^{y(1)} g(y') dy' = \int_0^1 f(x) dx$$

or

$$y(1) = \int_0^1 \sum e^{-\Sigma x} dx$$

Since $f(x)$ is a p.d.f., $y(x) \leq 1$. We can therefore let

$$N_r = y(1)$$

i.e., both the random number and the new stochastic variable $y(1)$ are distributed uniformly on the interval $(0,1)$. Now we see that a selection of N_r will determine l .

This brings in the Monte Carlo method of sampling a uniform distribution $g(y) = 1$ by selecting a random number between 0 and 1. We then have l in terms of the random number.

$$N_r = \int_0^1 \sum e^{-\Sigma x} dx = 1 - e^{-\Sigma l}$$

$$e^{-\Sigma l} = 1 - N_r$$

$$-\Sigma l = \ln(1 - N_r)$$

$$l = -\frac{1}{\Sigma} \ln(1 - N_r)$$

$$l = -\lambda \ln(N_r) \tag{3.1}$$

We have, in the latter equation, used the fact that $1 - N_r$ has the same distribution as N_r (namely uniform on the interval $(0,1)$) so sampling N_r is equivalent to sampling $1 - N_r$.

The distance traveled from one position to the next collision will for each case be found by equation (3.1) employing a "machine" generated random number N_r .

In order to find the position of the collision one must know whether or not it is for the first collision. If it is for the first collision, the following equations give its coordinates (see figure 5).

$$x = x_0 + l \sin \theta, \cos \varphi, \quad (3.2)$$

$$y = y_0 + l \sin \theta, \sin \varphi, \quad (3.3)$$

$$z = z_0 + l \cos \theta, \quad (3.4)$$

where $x_0, y_0, z_0, \theta, \varphi$ are the initial position and velocity direction coordinates.

If the collision is not the first we obtain the position by the equations

$$x' = x + l \sqrt{(\sin \theta' \cos \varphi' \cos \theta + \cos \theta' \sin \theta) \cos \varphi - \sin \theta' \sin \varphi' \sin \varphi} \quad (3.5)$$

$$y' = y + l \sqrt{(\sin \theta' \cos \varphi' \cos \theta + \cos \theta' \sin \theta) \sin \varphi + \sin \theta' \sin \varphi' \cos \varphi} \quad (3.6)$$

$$z' = z + l \cos \theta' \quad (3.7)$$

where $\sin \theta'$, $\cos \theta'$, $\sin \varphi'$ and $\cos \varphi'$ are determined by collision physics as discussed in subheadings 3.4 and 3.5.

After the collision position is determined a check is made whether it is still in the pile or not. If not, an "out" card is punched on which there is the initial weight, the final weight, the square of the final weight, and the numbers of collisions encountered with the various types of nuclei. If it remains in the pile at this new collision position, the type of target atom is determined. The following prescription is used to make the latter decision:

Let f_{Th} , f_O , f_H , and f_N stand for the probabilities of striking a thorium, oxygen, hydrogen or nitrogen atom respectively. Obviously they are conditional probabilities - conditional on there being a collision (the probability that there is a collision is one once we have determined l , the distance to the next collision). Then we have

$$f_{Th} + f_O + f_H + f_N = 1$$

and

$$f_{Th} = \frac{\sum_{Th}}{\sum_{i=1}^4 n_i \sigma_i} = \frac{n_{Th} \sigma_{Th}}{\sum_{i=1}^4 n_i \sigma_i} \quad (3.8)$$

$$f_0 = \sum_0 / \Sigma = n_0 \sigma_0 \left\{ \sum_{i=1}^4 n_i \sigma_i \right\}^{-1} \quad (3.9)$$

$$f_H = \sum_H / \Sigma = n_H \sigma_H \left\{ \sum_{i=1}^4 n_i \sigma_i \right\}^{-1} \quad (3.10)$$

$$f_N = \sum_N / \Sigma = n_N \sigma_N \left\{ \sum_{i=1}^4 n_i \sigma_i \right\}^{-1} \quad (3.11)$$

where all cross sections are determined for the incident neutron energy.

Now with a machine generated random number N_r we decide on an atom by using the Monte Carlo principle.

$0 \leq N_r < f_{Th}$	then thorium is the atom
$f_{Th} \leq N_r < f_{Th} + f_0$	then oxygen is the atom
$f_{Th} + f_0 \leq N_r < f_{Th} + f_0 + f_H$	then hydrogen is the atom
$f_{Th} + f_0 + f_H \leq N_r \leq 1$	then nitrogen is the atom.

It is now convenient to treat one of two possibilities:

- (1) The collision is not on thorium.
- (2) The collision is on thorium.

Case 1

For this case the only possible reaction is elastic scattering since in the energy range under consideration (10 ev. to 1000 ev.) the absorption cross sections are essentially zero for oxygen, hydrogen and nitrogen. The energy of the neutron following such a collision is selected again by the device of sampling from the supply of random numbers using the equation

$$E_2 = -E_1(1 - \alpha)N_r + E_1 . \quad (3.12)$$

This equation is based on the fact that all attainable energies following an elastic scattering are equally likely. See section 3.4, "The Collision", for the derivation of equation (3.12).

Case 2

If the collision occurs with thorium, the new weight* of the neutron is found by multiplying the pre-collision weight by the fraction scattered.

$$W_2 = W_1 \frac{\sigma_{sc}}{\sigma_{ab} + \sigma_{sc}} \quad (3.13)$$

where W_1 = pre-collision neutron weight

W_2 = after-collision neutron weight.

* Weight is used here in a statistical sense. For example, if n neutrons collide with n absorbers where each colliding pair has the same relative energy then if N are absorbed $\frac{n-N}{n}$ will be the fraction that scatter. Rather than give up a history when an absorption occurs we assign the above probability for scattering as a "weight" and continue the history.

The quantity in parenthesis is the fraction scattered. The thorium cross sections are determined using the expressions (4.10) and (4.11) which are derived in appendix II. The pre-collision energy is examined to determine within which peak it lies and whether the tabular values of $\psi(x,t)$ and $\chi(x,t)$ are to be used or if the asymptotic calculations are appropriate.

The history proceeds by going back through case 1 for a thorium scattering and if the post-collision energy is below 10 ev. a low energy card is punched with the same information as on the "out" card referred to earlier. If $E_2 > 10$ ev., the laws of conservation of momentum and kinetic energy require that the new direction be given by

$$\cos\theta' = \frac{1-A}{2} \sqrt{\frac{E_1'}{E_2}} + \frac{1+A}{2} \sqrt{\frac{E_2}{E_1}} \quad (3.14)$$

Subsection 3.4 with the subheading "The Collision" describes the latter equation and the energy selection in detail.

For the other velocity direction coordinate, ϕ' , as defined in figure 5 of section 3.5 we use the assumption of a uniform distribution for ϕ' and therefore use the sampling technique with the equation

$$\phi' = 2\pi N_r \quad (3.15)$$

After the sines and cosines of θ' and ϕ' are computed, the program returns to the computation of a new λ and λ' . The position of the next collision is determined by the equations (3.5), (3.6), and (3.7). This cycle is continued until all the source cards have been read.

A data-extraction program is used to sum the weights of neutrons starting a history, the weights of neutrons leaving the pile, the weights going to low energy ($E < 10$ ev.), and the various collision counts.

The programming details are presented in appendix IV.

3.2 Beginning a Neutron History

The initial information needed to start a history was obtained from a Monte Carlo model of water moderation for a pulsed source (21). The neutrons being produced by $H^2(H,n)H_e^3$ reaction. This program provides on an output card from the IBM-650 the position, energy, weight, and the direction of the velocity vector for a neutron the first time that its energy falls into the 990 ev. energy range from 10 ev. to 1000 ev.

In an attempt to provide an analytical method for starting histories, the above data cards were analyzed to determine radial probability distributions for various

values of the z coordinate which is parallel to the deuteron beam. The position integrated energy distribution of "first arrivals" turned out to be uniform between 10 ev. and 1000 ev. Sampling the position distributions and the energy separately seemed to be a good approach, but storing the additional data and program instructions appeared to require more storage than was available. The card-read method therefore was used. This limits the calculation for a given concentration to about 4300 histories.

Figure 2 indicates that $\bar{E}(z)$, the average energy per slab located at z , is essentially uniform. Tables 1, 2 and 3 show the various data that must be stored in the machine for future reference.

3.3 The Mean Free Path

For neutron energies below 1000 ev. we have only two significant neutron reactions occurring. They are radiative capture (n, γ) and elastic scattering. Other types are not energetically possible. The lowest energy levels of thorium are too high to be excited by these relatively low energy neutrons. Therefore \sum_{ab} (the absorption cross section) is all due to radiative capture and \sum_{sc} (the scattering cross section) is due only to elastic

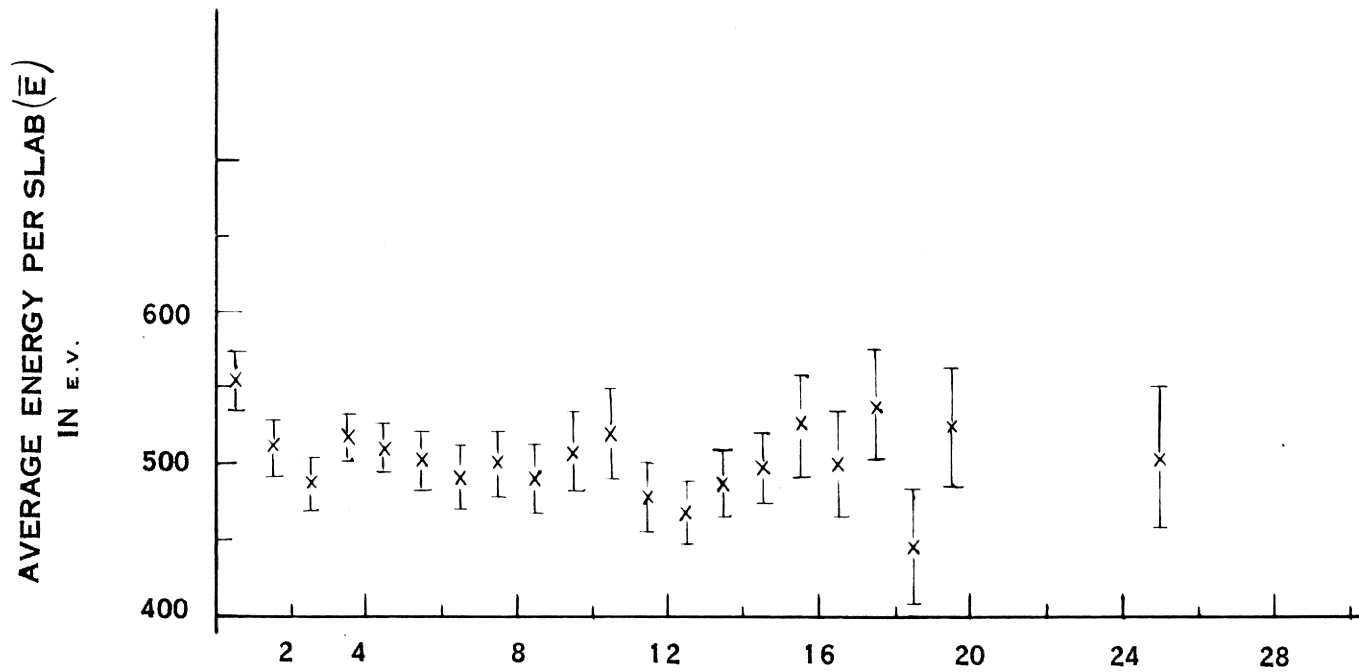


FIG. - 2

THE AVERAGE SOURCE ENERGY PER SLAB VERSUS Z

TABLE. 1

NUCLIDE NUMBER DENSITIES AND CROSSSECTION FOR FIVE CONCENTRATIONS OF TH(NO ₃) ₄ IN WATER.										
A / B	C	ρ GM/CM ³	$N_{TH} \times 10^{21}$ ATOMS/CM ³	$N_{OX} \times 10^{21}$ ATOMS/CM ³	$N_H \times 10^{21}$ ATOMS/CM ³	$N_N \times 10^{21}$ ATOMS/CM ³	σ_{OX} BARNs	σ_H BARNs	σ_N BARNs	\sum_{NOH} CM ⁻¹
	64.00	1.915	1.5381	41.51	46.10	6.152	3.8	20.2	9.1	1.145
1.2	45.45	1.580	0.9013	39.64	57.64	3.605	3.8	20.2	9.1	1.348
1.85	35.09	1.415	0.6231	38.91	61.43	2.492	3.8	20.2	9.1	1.411
3.00	25.00	1.272	0.3991	36.69	63.81	1.596	3.8	20.2	9.1	1.443
5.00	16.67	1.166	0.2439	35.42	64.99	0.976	3.8	20.2	9.1	1.456

TABLE. 1 USES THE FOLLOWING NOTATION: ρ = SOLUTION DENSITY, C = CONCENTRATION, A = MASS OF WATER USED FOR SOLUTION, B = MASS OF SALT DISSOLVED, N_{TH} = NUMBER OF THORIUM ATOMS PER UNIT VOLUME (N_{OX} , N_H AND N_N ARE THE SAME QUANTITY FOR OXYGEN, HYDROGEN AND NITROGEN RESPECTIVELY) σ_{OX} = MICROSCOPIC CROSSSECTION FOR NEUTRON INTERACTION WITH OXYGEN IN THE THORIUM RESONANCE REGION (σ_H AND σ_N ARE THE SAME QUANTITIES FOR HYDROGEN AND NITROGEN), $\sum_{NOH} = N_{OX} \sigma_{OX} + M_H \sigma_H + N_N \sigma_N$.

scattering. The total macroscopic cross section would then be

$$\sum_t = \sum_{ab} + \sum_{sc} \quad (3.16)$$

with
$$\sum_{ab} = \sum_{i=1}^{N=4} n_{i(i)} \sigma_{ab} \quad (3.17)$$

and
$$\sum_{sc} = \sum_{i=1}^{N=4} n_{i(i)} \sigma_{sc}. \quad (3.18)$$

Finally the mean free path becomes

$$\lambda = \frac{1}{\sum_t} = \frac{1}{\sum_{i=1}^4 (n_{i(i)} \sigma_{ab}) + n_{i(i)} \sigma_{sc}}. \quad (3.19)$$

The mean free path is energy-dependent because the cross sections are energy-dependent. It is therefore necessary to use the resonant behavior of thorium while computing λ .

As an example if one calculates λ for an "on resonance" thorium cross section and an "off resonance" value from peak 3 with $n_{Th} = 0.6231 \times 10^{21}$ atoms/cm³ there results

$$\lambda_{off} = .704 \text{ cm}$$

$$\lambda_{on} = .198 \text{ cm} .$$

So the mean free path for off the peak is about 3.6 times as large as the value at the peak maximum.

3.4 The Collision

The commoner method of handling the collision routine is, first, to sample the direction of travel after the collision from the known angular distribution of the elastic collision and then to determine the energy from conservation laws. The order of this procedure has been reversed in this paper since for elastic scattering the energy distribution is simpler to sample from and the calculation of direction, once the energy is known, is easy to perform on the "machine". We therefore begin with the energy determination.

Let E_2 = the neutron energy after collision

E_1 = the neutron energy before collision

$\alpha = \frac{A-1}{A+1}^2$ where A is the atomic mass of the target nucleus.

Experiments show the neutron scattering at energies of less than several Mev is spherically symmetric in the center of mass system. Therefore the probability of a neutron proceeding from a collision into solid angle $d\Omega$ formed by a conical element of angle θ and angular width $d\theta$ (see figure 3) is uniform, i.e.

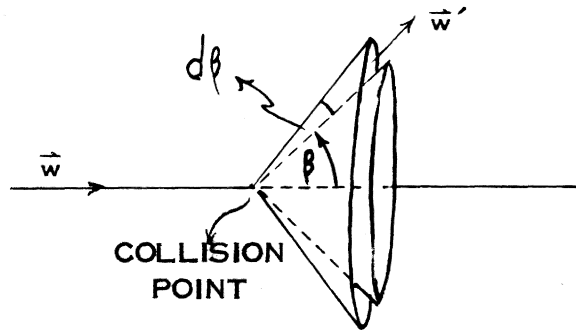


FIG. - 3. CENTER OF MASS COLLISION CONE.

- \vec{w} = THE CENTER OF MASS NEUTRON VELOCITY BEFORE COLLISION.
- \vec{w}' = THE CENTER OF MASS NEUTRON VELOCITY AFTER COLLISION.
- β = THE CENTER OF MASS ANGLE OF ELASTIC SCATTERING.

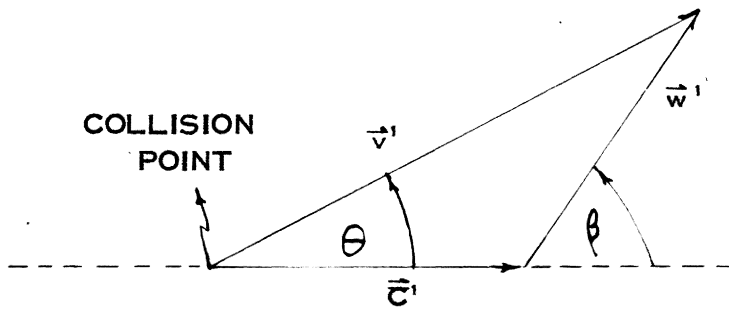


FIG. - 4. POST COLLISION NEUTRON VELOCITIES.

- θ = THE LABORATORY ANGLE OF ELASTIC SCATTERING.
- v' = THE NEUTRON VELOCITY IN THE LABORATORY.
- w' = THE NEUTRON VELOCITY IN THE CENTER OF MASS.
- c' = THE CENTER OF MASS VELOCITY.

$$\begin{aligned}
 p(\beta) d\beta &= \frac{d\Omega}{4\pi} = \frac{2\pi r \sin\beta r d\beta}{r^2} / 4\pi \\
 &= \frac{2\pi \sin\beta}{4\pi} d\beta = \frac{1}{2} \sin\beta d\beta
 \end{aligned}$$

$$\left| p(E_2) dE_2 \right| = \left| p(\beta) \right| \left| \frac{d\beta}{dE_2} \right| \left| dE_2 \right|$$

but
$$\frac{E_2}{E_1} = \frac{1}{2} \left[(1+\alpha) + (1-\alpha) \cos\beta \right] \tag{3.20}$$

see reference (7) from which we obtain

$$\left| \frac{d\beta}{dE_2} \right| = \frac{2}{E_1(1-\alpha) |\sin\beta|}$$

and
$$p(E_2) dE_2 = \frac{dE_2}{E_1(1-\alpha)} \tag{3.21}$$

Since $p(E_2)$ is then energy independent the distribution of E_2 is uniform and all values of E_2 are equally likely.

Now let

$$N_r = F(E_2) = \int_{E_2}^{E_1} P(E_2^1) dE_2^1$$

where $\alpha E_1 \leq E_2 \leq E_1$

$$N_r = \frac{(E_1 - E_2)}{E_1(1-\alpha)}$$

\therefore
$$E_2 = E_1 - E_1(1-\alpha) N_r \tag{3.22}$$

where N_r is again a random number ($0 \leq N_r \leq 1$) to be selected by the machine.

To complete the collision we need to have θ as a function of energy where θ is the scattering angle in the laboratory system corresponding to β , the scattering angle in the center of mass system.

From conservation of momentum and conservation of kinetic energy we have the equations:

$$\cos \theta = \frac{\frac{m}{M} \sqrt{\frac{2E_1}{m}} + \frac{A}{m} \sqrt{\frac{2E_1}{m}} \cos \beta}{\sqrt{\frac{2E_2}{m}}}, \quad M = m + A$$

$$\text{and } \cos \beta = \left(\frac{E_2}{E_1} - \frac{A^2 + m^2}{(A+m)^2} \right) \left[\frac{2mA}{(A+m)^2} \right]^{-1}$$

which combine to give for $m = 1$

$$\cos \theta = \frac{A+1}{2} \sqrt{\frac{E_2}{E_1}} - \frac{A-1}{2} \sqrt{\frac{E_1}{E_2}} \quad (3.23)$$

where A = target mass given in atomic mass units in the latter equation

m = neutron mass which equals 1 in atomic mass units

E_2 = neutron energy after collision in the laboratory system

E_1 = neutron energy before collision in the laboratory system.

Figure 4 shows the scattering angles in the two systems.

3.5 Tracking the Position

The initial space coordinates (x, y, z) and the velocity direction coordinates (θ, φ) , which are spherical coordinates with respect to the z axis as pole, are supplied as input data. The initial speed of the neutron is given indirectly by the neutron energy.

Referring to figure 5, the initial position which serves as origin for a second coordinate system $(\underline{x}, \underline{y}, \underline{z})$ parallel to (x, y, z) is given by the position vector \bar{R} . The initial flight direction is given by (θ_1, φ_1) . Still another set of axes (x', y', z') called the primed system is formed by making the z' axis a continuation of the pre-collision flight line l_1 . The x' axis is picked so as to be in the plane formed by \underline{z} and z' while y' is perpendicular to that plane. To make the selection unique we further require that the positive x' axis never intersect the positive \underline{z} axis.

Having calculated $\lambda(E)$ and l_1 by equations (3.19) and (3.1) we can find

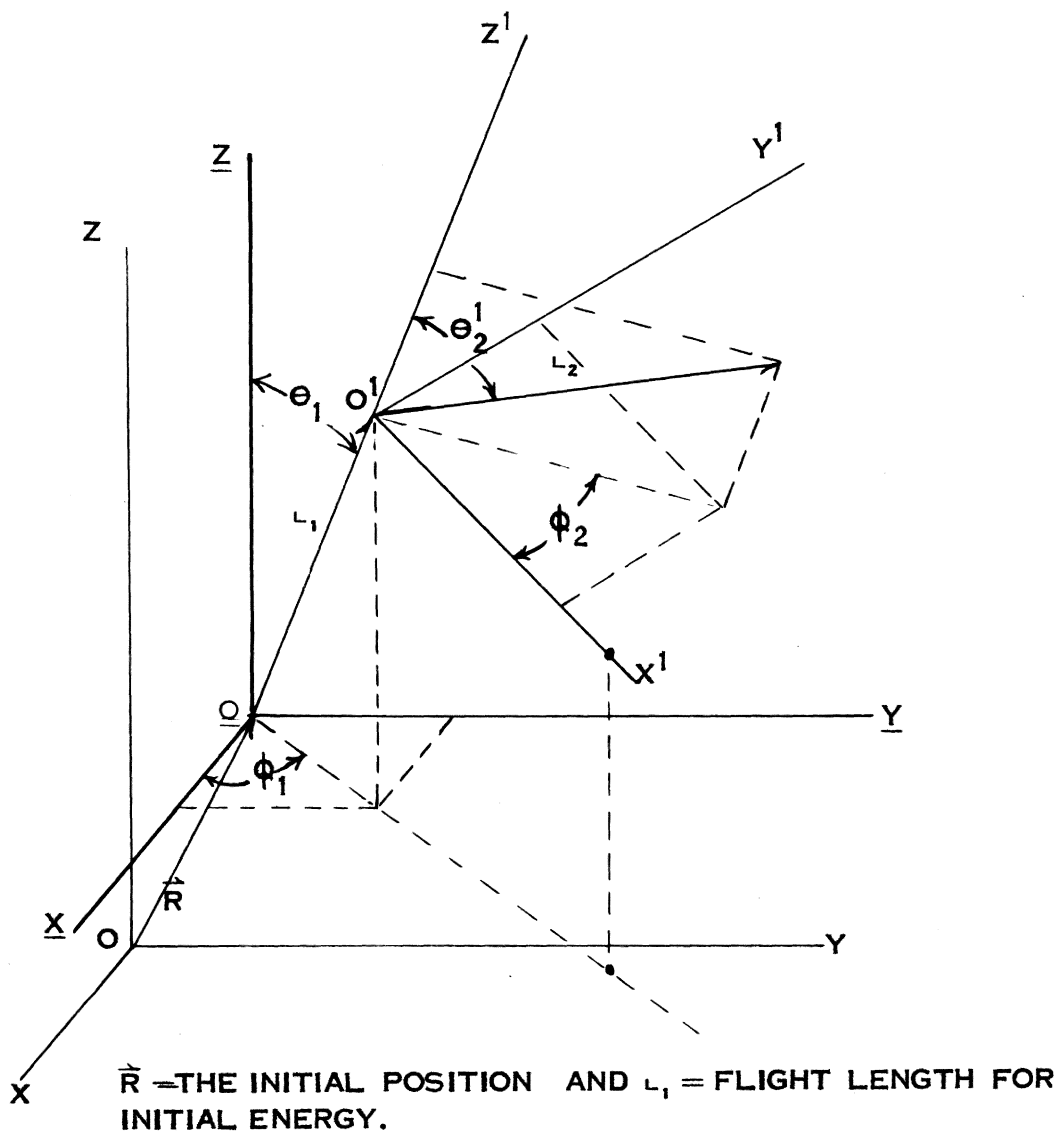


FIG. -- 5--

TRACKING COORDINATES

$$\underline{x} = \Delta x_1 = l_1 \sin \theta_1 \cos \varphi_1$$

$$\underline{y} = \Delta y_1 = l_1 \sin \theta_1 \sin \varphi_1$$

$$\underline{z} = \Delta z_1 = l_1 \cos \theta_1.$$

We now have the first collision position at O' given by

$$x_1 = x_0 + \Delta x_1$$

$$y_1 = y_0 + \Delta y_1$$

$$z_1 = z_0 + \Delta z_1$$

where $\bar{R} = x_0 \bar{i} + y_0 \bar{j} + z_0 \bar{k}$.

If the neutron at this new position is still in the pile, we proceed to find the position of the next collision. We have available both θ_2' and φ_2' by application of the Monte Carlo technique to the first collision. By application of equations (3.19) and (3.1) we obtain l_2 and then the primed coordinates become

$$\begin{pmatrix} x' \\ y' \\ z' \end{pmatrix} = \begin{pmatrix} l_2 \sin \theta_2' \cos \varphi_2' \\ l_2 \sin \theta_2' \sin \varphi_2' \\ l_2 \cos \theta_2' \end{pmatrix} .$$

Now by a coordinate rotation to the (x,y,z) system we have

$$\begin{pmatrix} \Delta x_2 \\ \Delta y_2 \\ \Delta z_2 \end{pmatrix} = \underline{M} \begin{pmatrix} x' \\ y' \\ z' \end{pmatrix} \quad (3.24)$$

where

$$\underline{M} = \begin{pmatrix} \cos\theta_1 \cos\phi_1 - \sin\phi_1 & \sin\theta_1 \cos\phi_1 \\ \cos\theta_1 \sin\phi_1 & \cos\phi_1 & \sin\theta_1 \sin\phi_1 \\ -\sin\theta_1 & 0 & \cos\theta_1 \end{pmatrix} .$$

The position of the second collision is then

$$\begin{aligned} x_2 &= x_1 + \Delta x_2 \\ y_2 &= y_1 + \Delta y_2 \\ z_2 &= z_1 + \Delta z_2 . \end{aligned}$$

A small saving in computer time due to leakage can be obtained if one waits until out checking starts before multiplying by l_2 . We, therefore, divide (3.24) by l_2 and define $A = \Delta x_2/l_2$, $B = \Delta y_2/l_2$, $C = \Delta z_2/l_2$, $a = x'/l_2$, $b = y'/l_2$, $c = z'/l_2$ to obtain

$$\begin{pmatrix} A \\ B \\ C \end{pmatrix} = \underline{M} \begin{pmatrix} a \\ b \\ c \end{pmatrix} . \quad (3.25)$$

The new collision location is then given by

$$(x_2, y_2, z_2) = (x_1 + l_2 A, y_1 + l_2 B, z_1 + l_2 C) . \quad (3.26)$$

The direction angles are then given by

$$\cos \theta_2 = C$$

$$\sin \theta_2 = \sqrt{1 - C^2}$$

$$\cos \varphi_2 = A / \sqrt{A^2 + B^2}$$

$$\sin \varphi_2 = B / \sqrt{A^2 + B^2} .$$

Since most of the leakage neutrons leave through the entrance face at $z=0$, the calculation for x_2 and y_2 may often be omitted if z is checked first. Hence, two multiplications are often saved, namely $l_2 A$ and $l_2 B$.

CHAPTER 4.

NEUTRON-NUCLEUS CROSS SECTIONS

In order to determine the fraction of the incident neutron weight that is scattered in a thorium encounter we must have some physical information to provide the probabilities of scattering and absorption. A common procedure is to describe the resonance cross section peaks by single level Doppler-Broadened Breit-Wigner equations which seem to apply quite well to thorium resonances. Cast in this form the cross sections are given by:

$$\sigma_{Th} = \sqrt{\frac{E'}{E_0}} \sigma_{or} \psi(x,t) + 4\pi R^2 + \sigma_{os} \psi(x,t) + \sqrt{\sigma_{pot} \sigma_{os}} \chi(xt) \quad (4.1)$$

where $\psi(x,t) = \frac{1}{2\sqrt{\pi t}} \int_{-\infty}^{\infty} \frac{e^{-(x-y)^2/4t}}{1+y^2} dy \quad (4.2)$

$$\chi(x,t) = \frac{1}{2\sqrt{\pi t}} \int_{-\infty}^{\infty} \frac{2ye^{-(x-y)^2/4t}}{1+y^2} dy \quad (4.3)$$

$$x = \frac{2}{\Gamma}(E-E_0), \quad y = \frac{2}{\Gamma}(E'-E_0) \quad (4.4) \quad (4.5)$$

$$t = \frac{4kTE_0}{A\Gamma^2} = 4.34 \frac{E_0}{\Gamma^2} \times 10^{-2} \quad (4.6)$$

$$\sigma_{or} = \frac{4\pi}{k_o^2} \frac{\Gamma_n \Gamma_\gamma}{\Gamma^2} = \frac{2.6 \times 10^6}{E_o} \frac{\Gamma_n \Gamma_\gamma}{\Gamma^2} \quad (4.7)$$

is the natural peak resonant absorption maximum cross section

$$\sigma_{os} = \frac{4\pi}{k_o^2} \frac{\Gamma_n^2}{\Gamma^2} = \frac{2.6 \times 10^6}{E_o} \frac{\Gamma_n^2}{\Gamma^2} \text{ ev. bns} \quad (4.8)$$

is the natural peak resonant scattering maximum cross section

$$\sigma_{pot} = 4\pi R^2 \quad (4.9)$$

is the hard sphere potential scattering cross section.

The other symbols used are defined as follows:

E_o = Energy corresponding to the maximum cross section for the resonance in ev.

R = effective nuclear radius

k = neutron wave number or propagation number corresponding to energy E

T = the temperature of the target particles or moderator nuclei

Γ_n = neutron level width

Γ_γ = radiation level width

Γ = total natural level width

$$\begin{aligned}
 k_0 &= \text{propagation constant for } E_0 \text{ neutron of} \\
 &\quad \text{energy } E_0 \\
 &= \frac{p_0}{\hbar} = \frac{2\pi}{\lambda_0} .
 \end{aligned}$$

The first term in equation (4.1) gives the resonant absorption cross section for the Doppler-broadened peak, and the next three terms together comprise the Doppler-broadened scattering cross section. Therefore we can write:

$$\sigma_{ab} = \sqrt{\frac{E_0}{E}} \sigma_{or} \psi(x,t) \quad (4.10)$$

for the thorium absorption cross section and

$$\sigma_{sc} = \sigma_{pot} + \sigma_{os} \psi(x,t) + \sqrt{\sigma_{pot} \sigma_{os}} \chi(x,t) \quad (4.11)$$

for the thorium scattering cross section.

The last two terms of the last expression form the resonant scattering cross section. The last term is often referred to as the interference term between the hard sphere (potential) scattering and the resonance scattering. For a more detailed development of equations (4.1) through (4.11) refer to appendix II.

The log σ vs. log E thorium resonance curves that appear in BNL-325 (reference 8) proved to be inadequate for the purposes of this paper. L. M. Bollinger (1) provided

the raw data, on which the above were based, in a form much easier to examine. These data were obtained at the Argonne National Laboratory with a fast chopper neutron spectrometer. Figures 6, 7, and 8 show portions of that data. The resolution for all measurements was about .09 usec/m which translates to 0.26 ev. for the lowest energy peak which is shown in figure 6. The theoretical fit at room temperature shown by the solid line is within the stated resolution as is the case for fits on the other peaks. The fits referred to were obtained by programming the IBM-650 to calculate equation (4.1). It is fortuitous that methods for extracting level parameters from transmission data have been developed that are independent of the detailed shape of the yield curve. Rosen (16) has used one such method known as area analysis to provide the thorium resonance parameters. His results corroborate those of Bollinger. With no available evidence to refute the Breit-Wigner peak shape detail we proceeded to apply equation (4.1) with Rosen's parameters for the lowest eight peaks. The function $\chi(x,t)$ was obtained by means of the relation

$$\chi(x,t) = 4t \frac{\partial \psi(x,t)}{\partial x} + 2x\psi(x,t) \quad (4.12)$$

where the derivative was taken graphically.

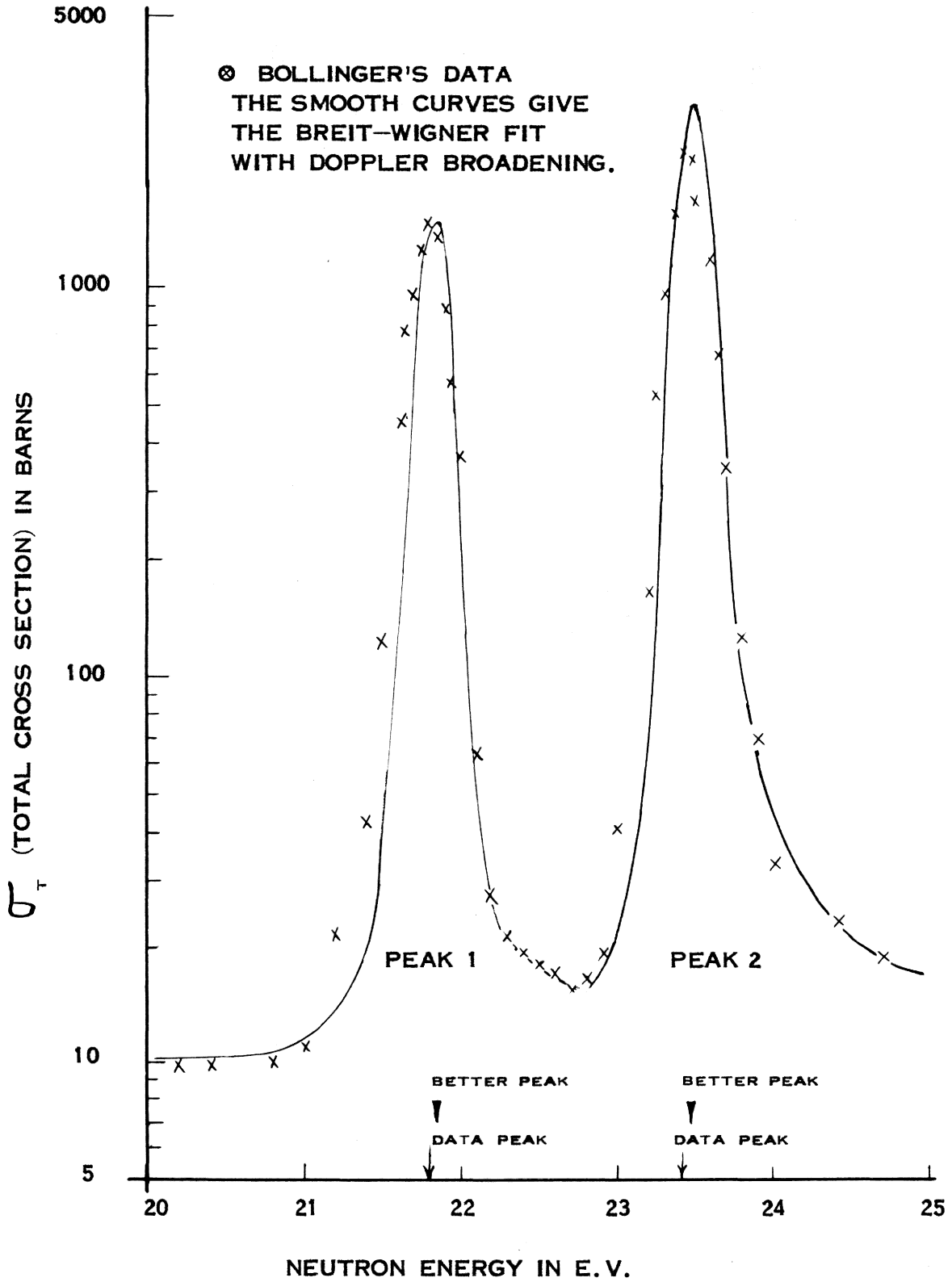


FIG. - 6
THORIUM RESONANCE PEAKS 1 AND 2.

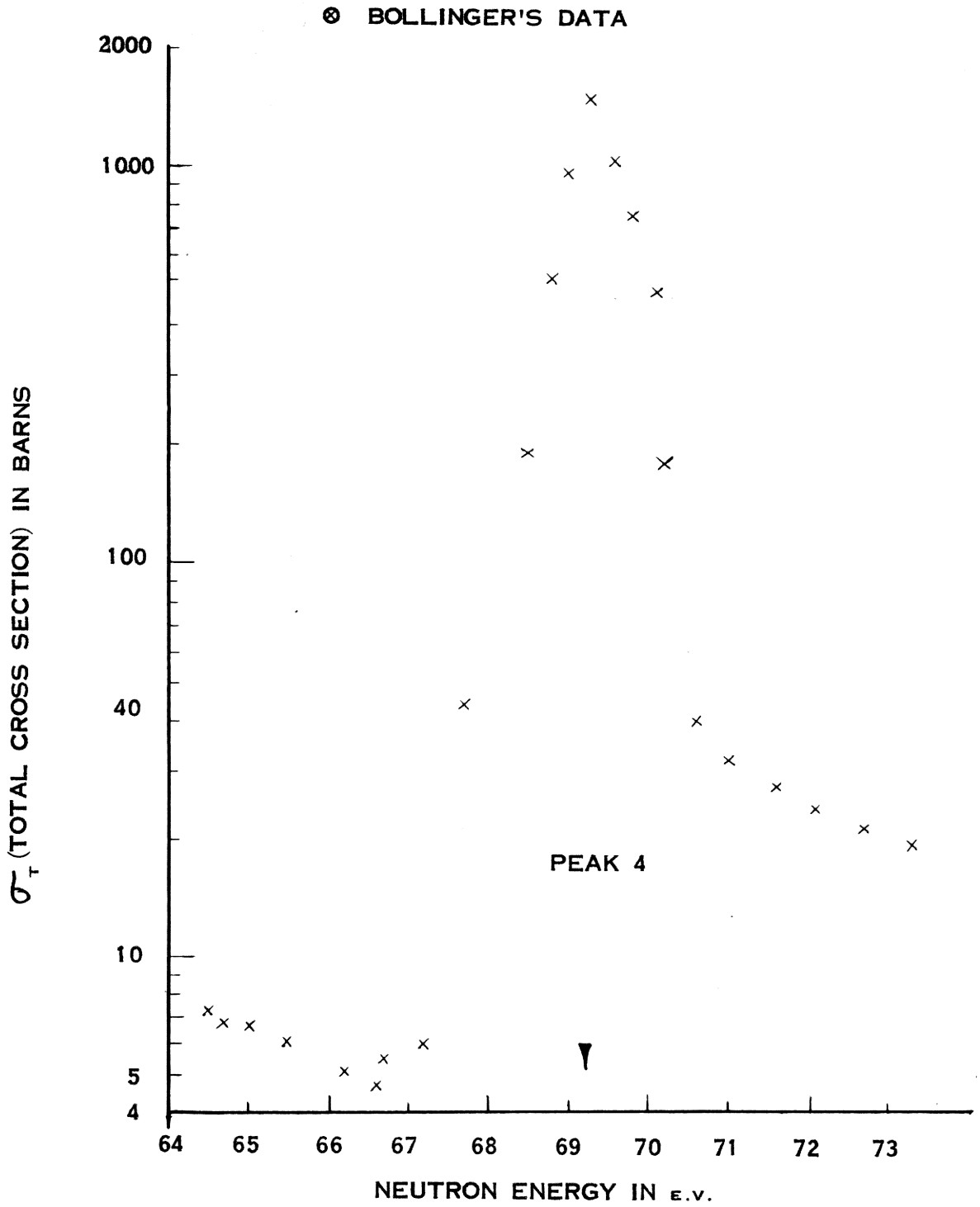


FIG. - 7
THORIUM RESONANCE PEAK 4.

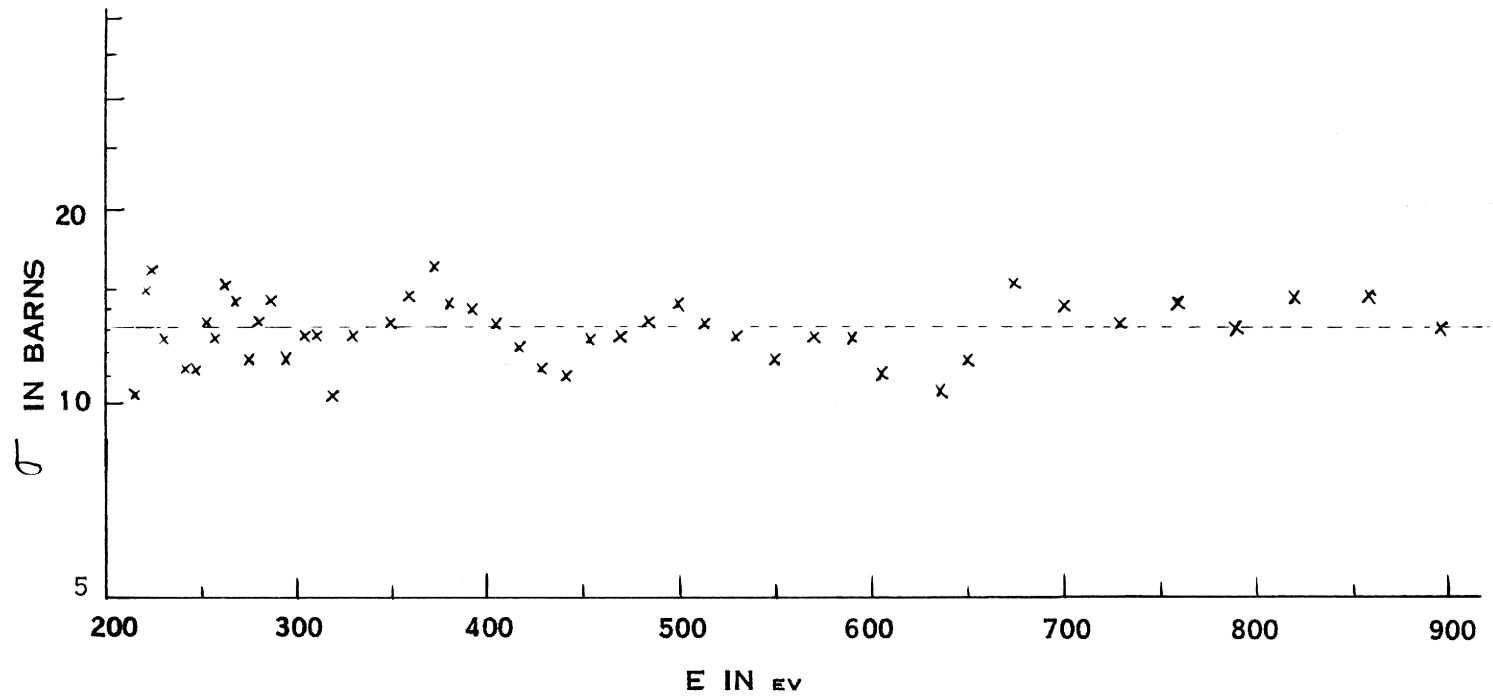


FIG. - 8. CROSS SECTIONS IN THE UNRESOLVED REGION.

To avoid excessively large machine storage tables of the functions $\Psi(x,t)$ and $\chi(x,t)$, asymptotic equations (given below) were used out in the wings of a resonance where $x^2 \gg t$. This compressed the tables down to about twenty entries per peak. The tabular procedure replaces the analytic function by a step function with what amounts to many steps over the peak. The asymptotic expressions used were:

$$\Psi(x,t) \simeq \frac{1}{1+x^2} \left[1 + \frac{2t(3x^2-1)}{(1+x^2)^2} + \dots \right] \quad (4.13)$$

$$\chi(x,t) \simeq \frac{2x}{1+x^2} \left[1 + \frac{2t(x^2-3)}{(1+x^2)^2} + \dots \right] \quad (4.14)$$

If more confidence could be placed in the available thorium cross section data, it would become reasonable to use smaller increments of x over the peak in order to approximate more closely the analytic function for the resonance. One must keep in mind however that this refinement coupled with a machine-generated source routine may well overload the IBM-650 storage capacity making access to a larger machine necessary. Also, there are resonances of small magnitude above the eight peaks treated, but their structure is not clear enough to incorporate in this calculation. An average value was used for these peaks. When

this structure is more accurately analyzed experimentally, one can easily add the corresponding parameters and functions to the program provided that sufficient machine storage is available. The variation of these higher energy peaks about the chosen average is very small and in most cases will contribute very little absorption. After all, ψ asymptotic is smaller than χ asymptotic so that σ_{sc} (resonance) is the largest contributor to the total cross section for energies far out in the wings. For the larger t 's of these high energy peaks, $\chi(x,t)$ is larger relative to $\psi(x,t)$ and hence the persistence of σ above σ_{pot} is largely due to the interference term of σ_{sc} .

CHAPTER 5.

COMPUTATIONS AND RESULTS

5.1 Resonance Escape

The theory of neutron slowing down processes for a homogeneous mixture of nuclides with hydrogen as the primary moderator leads to an expression for the slowing down density that contains the factor

$$\exp \left\{ - \frac{N_{Th}}{\xi \sum_s} \int_E^{E_0} \frac{\sigma_a(E') \sum_s(E')}{\sum_s(E') + \sum_a(E')} \frac{dE'}{E'} \right\} .$$

If one defines a resonance escape probability by the relation:

$$p(E; E_0) = \frac{q(E)}{q(E_0)} \quad (5.1)$$

where $q(E)$ = the slowing down density at energy E
 $q(E_0)$ = the number of neutrons leaving the source at energy E_0 per cm^3 per sec

$$\text{then } p(E, E_0) = \exp \left\{ - \frac{N_{Th}}{\xi \sum_s} I_{\text{eff}} \right\} \quad (5.2)$$

$$\text{where } I_{\text{eff}} = \int_E^{E_0} \frac{\sigma_a(E') \sum_s(E')}{\sum_s(E') + \sum_a(E')} \frac{dE'}{E'} . \quad (5.3)$$

A more complete discussion of these relations appears in reference (12).

If there is no absorption for $E \geq E_1$, where the resonance region is defined by $E_2 \leq E \leq E_1$, then

$$P(E_2:E_1) = P(E_2:E_0) = \frac{q(E_2)}{q(E_0)} . \quad (5.4)$$

When hydrogen is present in the mixture the possibility exists that a neutron can skip the resonance region with one collision on hydrogen. Definition (5.4) counts such events in both $q(E_2)$ and $q(E_1)$. We wish to exclude such events from our probability as implied by the definition offered in the introduction where the number of neutrons skipping is deleted from both $q(E_2)$ and $q(E_1)$ by the phrases "...from the resonance region..." and "...enter that region from above 1000 ev.".

The probability excluding "skipping" will be reported as REP_∞ and REP_g for the infinite and finite geometry cases respectively. The probability including "skipping" will be reported as REP'_∞ and REP'_g for the same two geometry cases.

The following information can be obtained as output data for a complete calculation:

W_1 = the sum of the weights attaining low energy
from the resonance energy region

W_{in} = the sum of the weights of the source neutrons each of which starts with energy in the resonance region

W_o = the sum of the neutron weights that leak through the walls of the container and go out of the pile.

The quantity W_s (the sum of the weights skipping the resonance region) is obtained from the first stage Monte Carlo developed by Settles (21). It then follows that we have

$$REP_g = \frac{W_1}{W_{in}} , \quad REP'_g = \frac{W_1 + W_s}{W_{in} + W_s} \quad (5.5), (5.6)$$

$$REP_\infty \simeq \frac{W_1}{W_{in} - W_o} , \quad REP'_\infty \simeq \frac{W_1 + W_s}{W_{in} - W_o + W_s} \quad (5.7), (5.8)$$

Equation (5.8) should come closest to providing a value of

$$P(E_2 : E_1) = \exp \left\{ - \frac{M_{Th}}{\xi \sum s} I_{eff} \right\} .$$

Equation (5.7) comes about because

$$REP_\infty \simeq \frac{W_1 + (REP_\infty)W_o}{W_{in}} .$$

Reference to tables 4 and 5 will show the escape probabilities determined by the Monte Carlo program for

TABLE. 4.

DATA FROM OUTPUT CARDS									
N_{TH} $\times 10^{21}$ $\frac{ATOMS}{CM^3}$	$W_{IN} =$ $\sum_i W_{IN}$	$W_{LOW} =$ $\sum_i W_{LOW}$	$\sum_i W_{LOW}^2$	$W_{OUT} =$ $\sum_i W_{OUT}$	N_N	N_C	N_H	N_{OX}	N_{TH}
1.5381	4317.475	3836.553	3787.629	258.012	1082	23533	18656	3121	674
.9013	4316.475	3940.634	3908.280	230.550	550	22230	18852	2466	362
.6231	4315.480	4008.910	3985.000	214.129	390	21741	18882	2232	237
.3991	4212.490	3941.890	3922.120	194.750	252	21152	18617	2111	172
.2439	4316.480	4073.150	4062.830	198.750	141	21381	19091	2038	103

1 104 OUTPUT CARDS WERE ACCIDENTLY LOST. THEREFORE WITH $\frac{21152}{3213} =$
 5.02 COLLISIONS PER CARD AN ADDITIONAL 104 CARDS AUGHT TO
 INCREASE N_C BY $104 \times 5.02 = 523$ COLLISIONS SO THAT $N_C = 21675$
 COLLISIONS. THIS MAINTAINS THE INCREASE OF N_C WITH N_{TH} .

TABLE. 5

PROBABILITY RESULTS										
$N_{TH} \times 10^{-21}$ ATOMS/CM ³	REP _G	REP _∞	REP' _G	REP' _∞	P _{OX}	P _H	P _N	P _{TH}	P _{AB}	P _{AB}
.2439	.9436	.9892	.9443	.9893	.0953	.8929	.0066	.0048	.437	.4260
.3991	.9358	.9811	.9366	.9814	.0998	.8802	.0119	.0081	.441	.4535
.6231	.9290	.9775	.9298	.9778	.1027	.8685	.0179	.0109	.390	.3945
.9013	.9129	.9644	.9140	.9649	.1109	.8480	.0247	.0165	.4014	.4130
1.5381	.8886	.9451	.8900	.9458	.1326	.7932	.0460	.0286	.3298	.3285

various thorium number densities. Figure 10 displays these results graphically.

A five point least squares fit to a straight line was made for the REP_∞ curve with the result that

$$P = \text{REP}_{\infty} = 1 - .0367n \quad (5.9)$$

where n is the thorium number density in atoms per cm³. The closeness of the fit can be seen by comparing the observed data points to those calculated by equation (5.9) as listed in table 13.

To decide whether the data is sufficiently well fit by a straight line rather than by a higher degree polynomial a quadratic fit was made giving the equation

$$P = 1 - .03669n + .005095n^2 \quad (5.10)$$

A test to measure improvement employs the F statistic given by

$$F(K, n-k) = \frac{\sum_{i=1}^n l^e_i{}^2 - \sum_{i=1}^n q^e_i{}^2}{\frac{\sum_{i=1}^n q^e_i{}^2}{n-k}}$$

where l^e_i = the deviation of the ith data point from the linear curve

q^e_i = the deviation of the ith data point from the quadratic curve

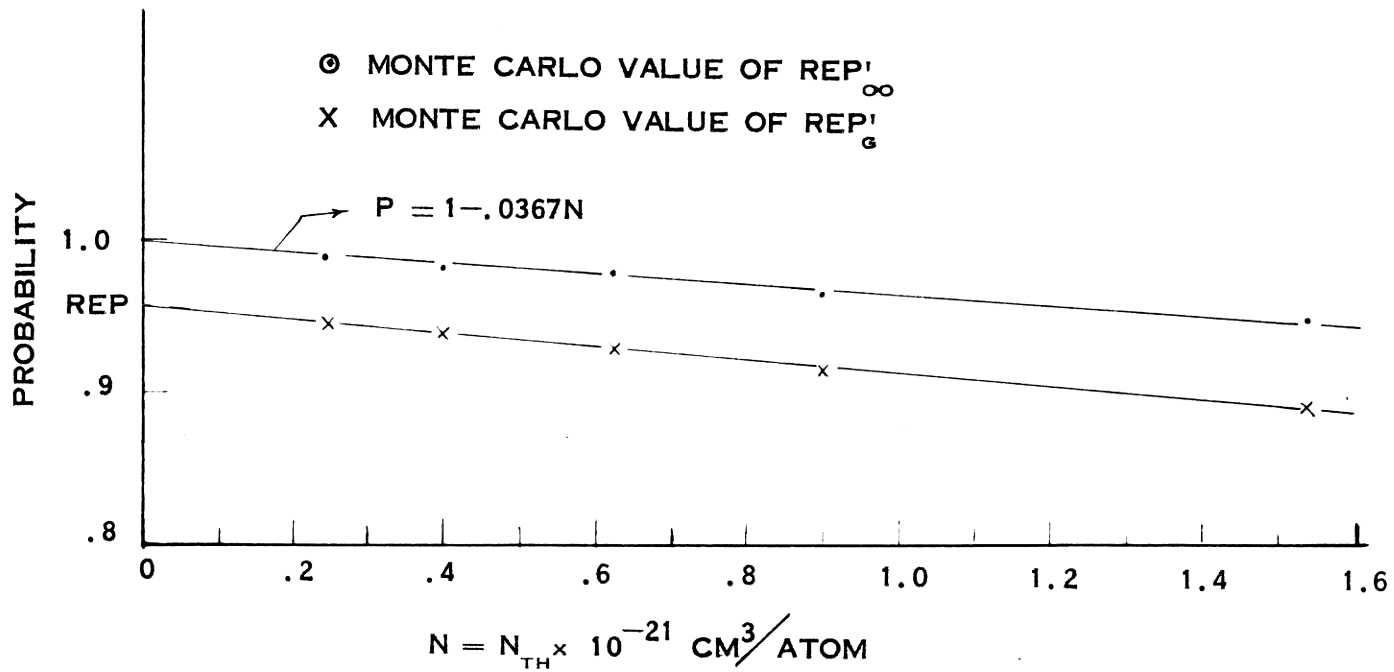


FIG. - 10

RESONANCE ESCAPE PROBABILITY AS A FUNCTION OF THORIUM
 NUMBER DENSITY

- n = the number of data points
- k = the number of degrees of freedom in the quadratic case
- K = the number of degrees of freedom in the linear case.

For our problem $n = 5$, $k = 2$, $K = 1$, and $F(1,3) = 3.85$.

From a table of the F distribution we find

$$\begin{aligned}F_{.10}(1,3) &= 5.54 > 3.85 \\F_{.05}(1,3) &= 10.13 > 3.85 \\F_{.01}(1,3) &= 34.12 > 3.85.*\end{aligned}$$

We conclude, therefore, that at all levels of significance the linear model fits the data and that the error reduction due to the quadratic term is insignificant. Equation (5.9) gives the functional dependence of P on n sufficiently well.

The separate contributions to the reduction of the resonance escape probability by the effects of leakage and absorption are displayed for comparison in table 6. The increase in the leakage effect with larger n_{Th} is to be expected since, with the addition of more $Th(NO_3)_4$, the

* This notation means that the chance for $F > 5.54$ is 0.1 or the fraction of the area under the F frequency function beyond $F = 5.54$, i.e.,

$$\text{for } \int_0^{\infty} f(F)dF = 1 \quad 0.1 = \int_{5.54}^{\infty} f(F)dF.$$

TABLE. 6

COMPARISON OF LEAKAGE AND ABSORPTION		
$N_{TH} \times 10^{-21}$ ATOMS/CM ³	% LEAKAGE ($REP_{\infty} - REP_G$)	% ABSORPTION ($1 - REP_{\infty}$)
.2439	4.26	1.08
.3991	4.53	1.89
.6231	4.85	2.25
.9013	5.15	3.56
1.5381	5.65	5.49

TABLE. 7

NUCLIDE POPULATION CONTROL OF \sum_{NOH}			
$N_{TH} \times 10^{-21}$ ATOMS/CM ³	$N_{OX} \times 10^{-21}$ ATOMS/CM ³	$N_H \times 10^{-21}$ ATOMS/CM ³	\sum_{NOH} IN CM ⁻¹
.2439	35.42	64.99	1.456
.3991	36.69	63.81	1.433
.6231	38.91	61.43	1.409
.9013	39.64	57.64	1.348
1.5381	41.51	46.10	1.145

relative number density of hydrogen will be less. With the heaviest contribution to the total macroscopic cross section coming from hydrogen we expect that cross section to reduce along with the hydrogen number density and therefore produce larger mean free paths.

$$\lambda = \frac{1}{n_{\text{Th}} \sigma_{\text{Th}} + n_{\text{ox}} \sigma_{\text{ox}} + n_{\text{N}} \sigma_{\text{N}} + n_{\text{H}} \sigma_{\text{H}}} \quad (5.10)$$

We have values of the sum

$$\sum_{\text{NoH}} = \sum_{\text{ox}} + \sum_{\text{N}} + \sum_{\text{H}} \quad (5.11)$$

for the five values of n_{Th} . We see from table 7 that they decrease with increasing n_{Th} .

5.2 Collision Probabilities

We notice that the last point for each graph of figure 11 deviates from the approximate linear pattern set by the points for small n_{Th} . We can expect relatively more collisions with thorium because of multiple collisions that are infrequent on the smaller samplings of thorium collisions, but we would expect to see some multiple collisions on the larger samplings that go with larger n_{Th} .

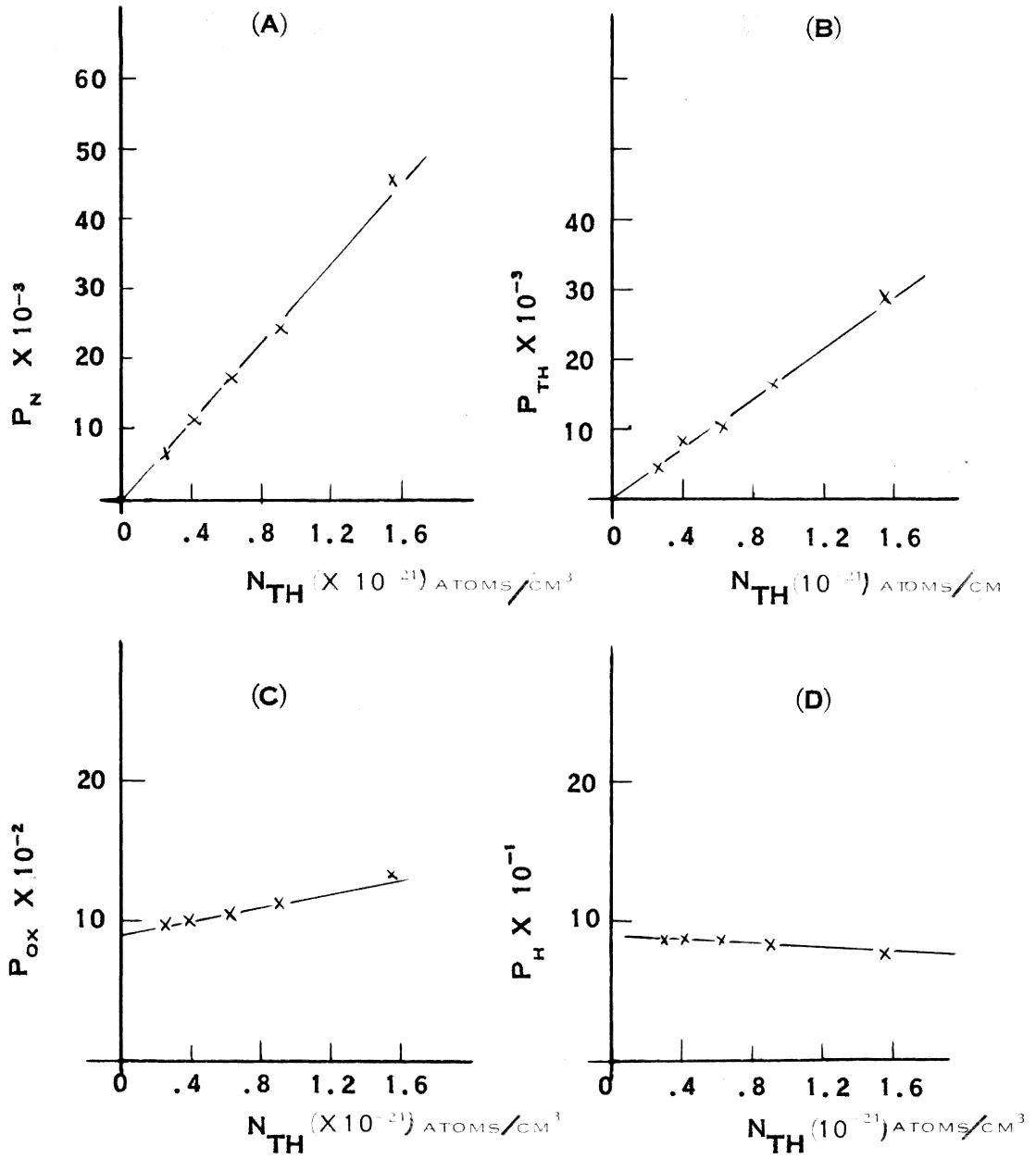


FIG. - 11

ATOMIC COLLISION FREQUENCIES

(A) NITROGEN (B) THORIUM (C) OXYGEN (D) HYDROGEN

Whereas, n_N and n_{Ox} increase faster than linear with a linear increase of n_{Th} making possible a faster than linear increase of their collision frequencies. Accompanied with this, we get a faster than linear decrease in n_H making possible a faster than linear decrease in its collision frequency with n_{Th} . These latter effects are due to the non-linearity shown in figure 12. See equations in appendix III.

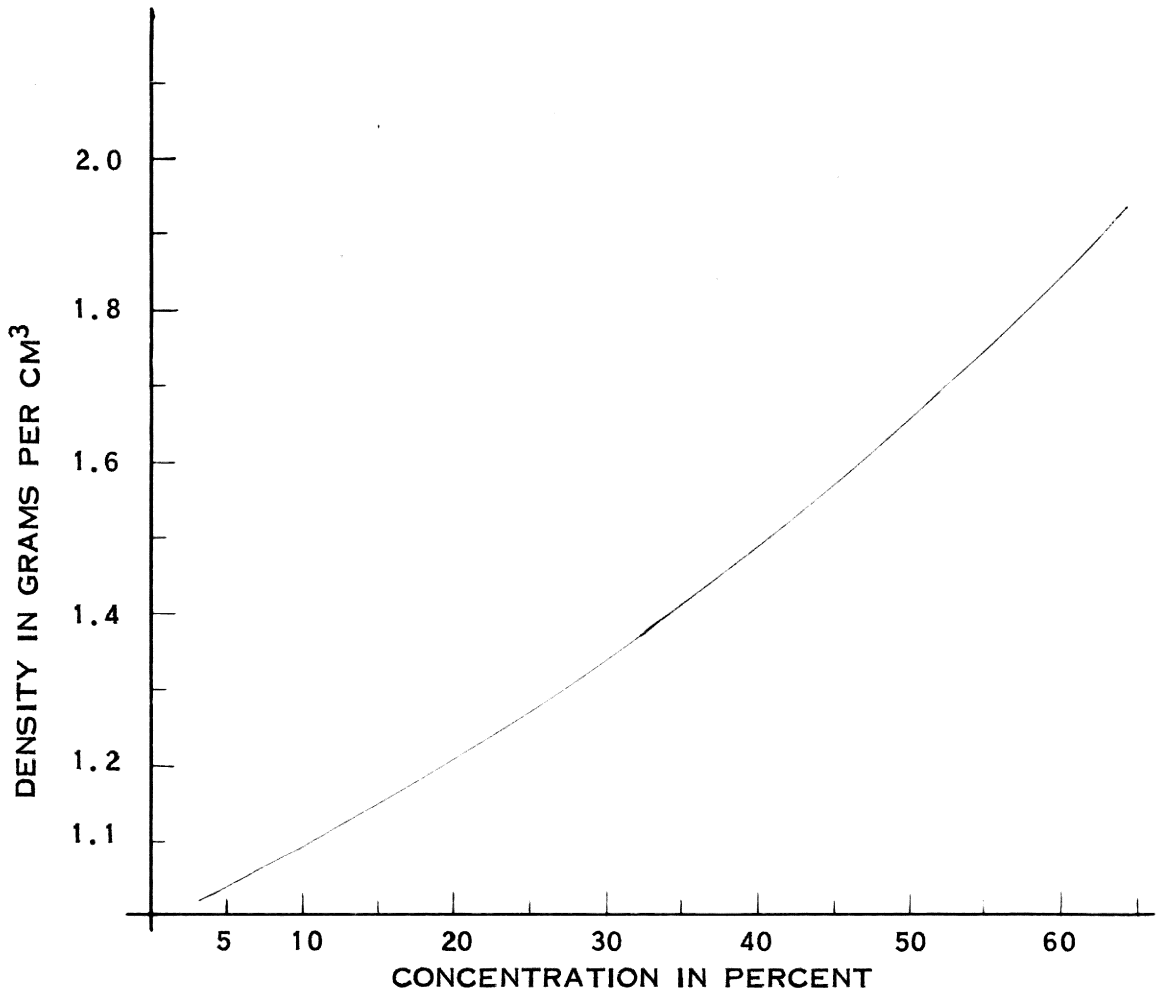


FIG. - 12

DENSITY AT 20°C OF TH(NO₃)₄ AQUEOUS SOLUTION AS A FUNCTION OF CONCENTRATION

CHAPTER 6.

ERROR ANALYSIS AND CONCLUSIONS

6.1 Monte Carlo Statistics

The random error or measure of statistical variation can be estimated by means of the central limit theorem which for the case of weighted events takes the form

$$P \left(\left| \frac{M}{N} - a \right| < \epsilon \right) = \text{erf} \left(\frac{t}{\sqrt{2}} \right) + \rho_N \quad (6.1)$$

where $t = \epsilon \sqrt{\frac{N}{b}}$ and $\rho_N \rightarrow 0$ as $N \rightarrow \infty$

b = the dispersion

$\frac{M}{N}$ = the ratio of the number of histories surviving to below 10 ev. to the number of histories begun

a = true value of the escape probability.

We take as an estimator of b the quantity β which is given by:

$$\beta = \sum_{i=1}^N \frac{(w_{1i})^2}{w_{in}} - \left(\frac{w_1}{w_{in}} \right)^2$$

$$\beta = \overline{w^2} - \bar{w}^2 \quad (6.2)$$

The error function

$$\text{erf}(x) = \frac{2}{\sqrt{\pi}} \int_0^x e^{-x'^2} dx' \quad (6.3)$$

is well tabulated.

If we wish to specify a probability of 0.5 that the computed REP be within $\pm \epsilon$ of the correct value a we must then pick an $\epsilon > 0$ such that $\text{erf}\left(\frac{t}{\sqrt{2}}\right)$ is about 0.5. We will refer to such an ϵ as the probable error. For this to be true $\frac{t}{\sqrt{2}} \approx .5$ hence $\epsilon \sqrt{\frac{W_{in}}{2b}} = .5$

or
$$\epsilon = \frac{1}{2} \sqrt{\frac{2b}{W_{in}}}$$

Now
$$\bar{W} = \frac{\sum_i W_{in,i} W_{1,i}}{\sum_i W_{in,i}}$$

however a very good estimator of this number is

$$\bar{W} = \frac{W_1}{N}$$

since all $W_{in,i}$ are about equal to unity. We then have

$$\beta = \frac{\sum_{i=1}^N (W_{1,i})^2}{N} - \left(\frac{W_1}{N}\right)^2 \quad (6.4)$$

The results with ϵ displayed as the probable error are given in table 8.

TABLE. 8

RESULTS INCLUDING MONTE CARLO STATISTICAL
PROBABLE ERRORS

$N_{TH} \times 10^{21}$ ATOMS/CM ³	REP. %	PROBABLE ERROR	PERCENT ERROR
1.5381	.9458	.0026	.27
.9013	.9649	.0018	.19
.6231	.9778	.0014	.14
.3991	.9814	.0013	.13
.2439	.9893	.0010	.10

6.2 Probable Error for the Slope of Equation (5.9)

We wish to estimate the probable error of the slope of the equation

$$P = 1 - .0367n .$$

Assume an equation

$$P = 1 + an . \quad (6.5)$$

The following procedure leads to the normal equations of a least squares fit:

$$v_i = P_i - (1+an_i)$$

$$\sum_i^N v_i^2 = \sum_i^N [P_i - (1+an_i)]^2$$

$$\frac{\partial \sum_i^N v_i^2}{\partial a} = 0 = \sum_i^N 2 [P_i - (1+an_i)] (-n_i)$$

$$\text{or } \sum_i^N [P_i - (1+an_i)] n_i = 0 . \quad (6.6)$$

This last set of equations is the normal equations.

$$(P_1 n_1 - n_1 - a n_1^2) + (P_2 n_2 - n_2 - a n_2^2) + \dots = 0$$

hence
$$\sum_{i=1}^5 P_i n_i - \sum_{i=1}^5 n_i = a \sum_{i=1}^5 n_i^2$$

or
$$a = \frac{\sum_i P_i n_i - \sum_i n_i}{\sum_i n_i^2} . \quad (6.7)$$

If one considers the n_i fixed constants and the P_i variables then we can write an equation for the probable error.

$$\epsilon_a = \sqrt{\sum_{i=1}^N \left(\frac{\partial a}{\partial P_i} \epsilon_{P_i} \right)^2} \quad (6.8)$$

or
$$\epsilon_a = \frac{\sqrt{\sum_{i=1}^5 (n_i \epsilon_{P_i})^2}}{\sum_i n_i^2} . \quad (6.9)$$

For the Monte Carlo results we have the values listed in table 9 whence we obtain

$$\epsilon_a = \frac{\sqrt{19.7118 \times 10^{-6}}}{3.7698} = \frac{4.4398 \times 10^{-3}}{3.7698} = 1.1777 \times 10^{-3}$$

and we then have

$$\begin{aligned} a &= -(0.0367 \pm 0.0012) \\ &= -0.0367(1 \pm 0.033) . \end{aligned}$$

TABLE. 9

QUANTITIES FOR SLOPE PROBABLE ERROR

N_I	N^2	$\epsilon_{PI} \times 10^{-3}$	$N_I \epsilon_{PI} \times 10^{-2}$	$(N \epsilon_P)^2 \times 10^{-8}$
1.5381	2.3504	2.6	4.00	1600.00
.9013	0.8123	1.8	1.62	262.44
.6231	0.3883	1.4	8.72	76.04
.3991	0.1593	1.3	5.19	26.94
.2439	0.0595	1.0	2.40	5.76

6.3 Built-In Systematic Errors

The model provides no absorption in the energy region where the cross section is fit with the exponential function

$$\sigma_{Th} = 33.78 e^{-0.01113E} \quad (6.10)$$

where $76 \text{ ev.} < E \leq 105 \text{ ev.}$

This is a very good approximation since the resonance absorption due to the 69.20 ev. resonance drops off much more rapidly than the resonance scattering for that peak, i.e., the interference term in σ_{Th} controls the variation in the interval in question.

The model also neglects absorption in the interval $185.5 \text{ ev.} < E < 1000 \text{ ev.}$ where an average of 13.2 barns has been used. This latter number came from Bollinger's raw data (1) parts of which are displayed graphically in figures 6, 7, and 8. The resonance structure of the region is neglected since the data is quite uncertain and the contributions from absorption are very small in general compared to the total of potential scattering, resonant scattering, and interference. The interference and potential terms are completely dominant in the wings of these relatively weak and poorly resolved resonances since $\chi(x,t)$ decreases more slowly than the function $\psi(x,t)$ which controls the resonant absorption and scattering.

6.4 Discussion of the Results

Probably the most striking feature of the Monte Carlo results is the "goodness of fit" to a straight line for resonance escape probability as a function of thorium number density. In view of the very small probable errors for each REP determination we conclude that more than a sufficient number of histories were processed to provide "good statistics".

Although we might expect no change in the probability for an absorption (given that a thorium interaction occurs) from density to density, nevertheless, the data seen in table 5 and figure 13 for P_{ab} , show considerable fluctuations on top of a general downward trend with increasing n_{Th} . We do, of course, expect the variation since the statistics (in this case the total weight absorbed) are much poorer than for the REP calculations. One would have to process about twenty times as many histories to provide similarly precise data for P_{ab} . We might explain the downward trend of P_{ab} , with increasing n_{Th} on the basis that \sum_{Th}/Σ increases. One recalls that it is this ratio which, according to the Monte Carlo prescription of section 3.1, controls the selection of thorium for a collision. For the first collision of a history, the probability of

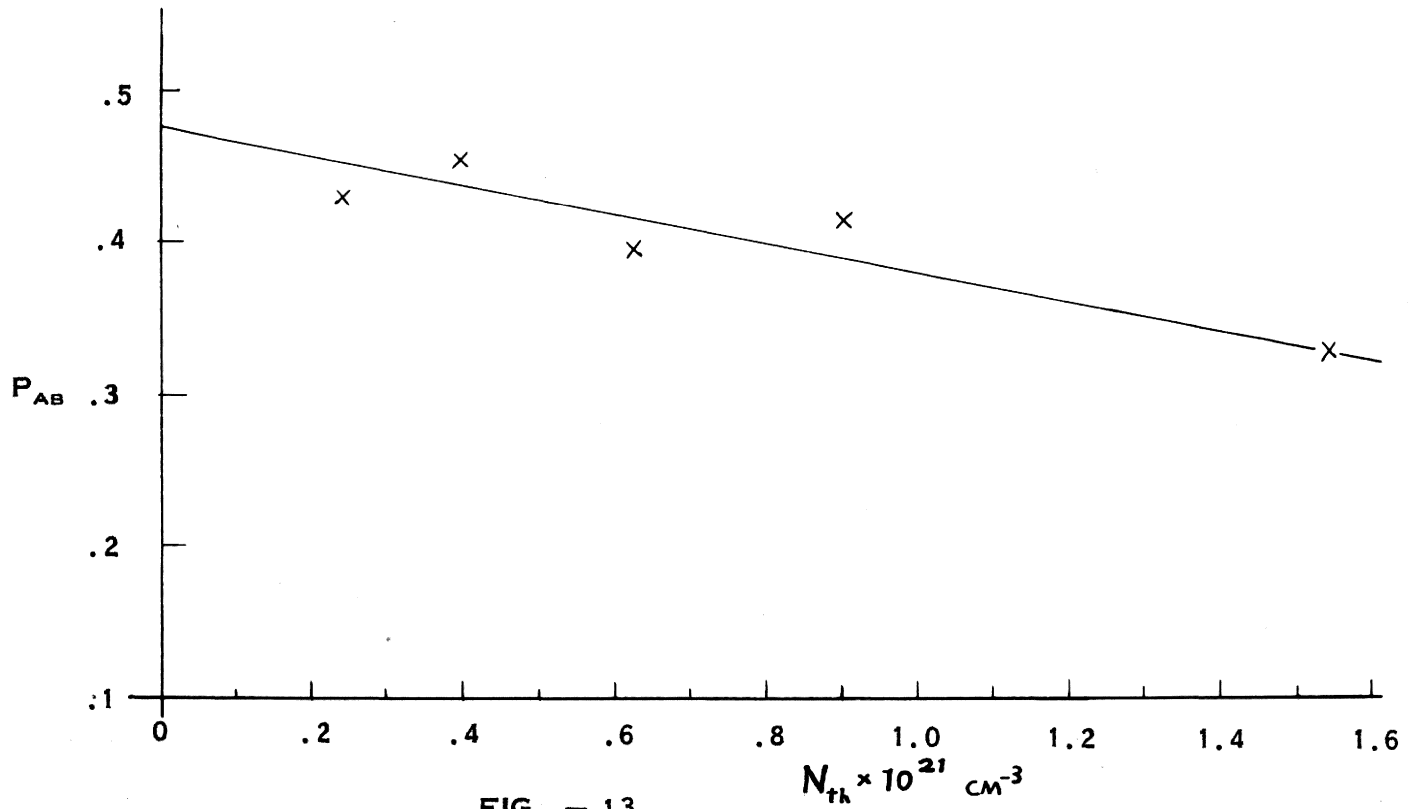


FIG. - 13

PROBABILITY FOR AN ABSORPTION GIVEN A THORIUM COLLISION

a thorium collision will be larger if $\frac{\sum_{Th}}{\sum}$ is larger.

Since

$$\frac{\sum_{Th}}{\sum} = \frac{1}{1 + \frac{\sum_{NoH}}{\sum_{Th}}}$$

we can examine $\frac{\sum_{NoH}}{\sum_{Th}}$ for the answer. We note in table 5 that \sum_{NoH} decreases with increasing n_{Th} and that $\sum_{Th} = n_{Th} \sigma_{Th}$ is in general larger for larger n_{Th} . Therefore the ratio $\frac{\sum_{NoH}}{\sum_{Th}}$ is smaller, making the ratio $\frac{\sum_{Th}}{\sum}$ larger. This means that for a run with larger n_{Th} relatively more thorium collisions occur at higher neutron energies where the absorption cross sections are smaller. This reduces the amount of absorption per thorium collision on the average.

The percentage of leakage increases with n_{Th} indicating longer mean free paths in general. Since

$$\sum = \sum_{Th} + \sum_{NoH},$$

we conclude that the decrease in \sum_{NoH} is not compensated by the increase in \sum_{Th} . The reduction of \sum_{NoH} may appear to be at odds with the idea that a more dense solution should increase its value. However, the element of highest cross section is hydrogen and its density decreases with increasing concentration by enough to reduce the overall value of \sum_{NoH} .

6.5 Comparisons to Analytical Calculations

The analytical evaluation of REP is very difficult for the whole resonance region as one problem. Calculating a REP for even one resonance can be quite laborious. A qualitative discussion of the problem is useful.

It is important to distinguish between wide resonances and narrow resonances by stating a criterion for the classification. It may seem paradoxical but a resonance with a width large compared to another can be classified narrower by use of the criterion. For example, with a criterion that $\Gamma_1 \ll E_1(1-\alpha)$ where E_1 is an energy above the i^{th} resonance, there will be fewer neutron reactions in the resonance, i.e., the width is narrow compared to the energy change that can accompany a scattering. The figure 14 indicates the concept. $\Delta E_{\text{max}} = E_1(1-\alpha)$ and the smaller is $\Gamma/\Delta E_{\text{max}}$, the narrower is the peak.

If E_0 is large then $E_1 \simeq E_0$ and $\Delta E_{\text{max}} \simeq E_0(1-\alpha)$. For a specific example let us try to decide which is the wider of two thorium resonances. We shall pick the $E_0 = 21.84$ ev. and the $E_0 = 170.80$ ev. resonances from table 2 where they are labeled peak 1 and peak 8.

$$\begin{aligned} \Gamma_1 &= \frac{2.00}{55.55} \text{ ev.} = .036 \text{ ev.}, & \Gamma_8 &= \frac{2.00}{18.87} \text{ ev.} = .106 \\ &= 36 \text{ mv} & &= 106 \text{ mv} . \end{aligned}$$

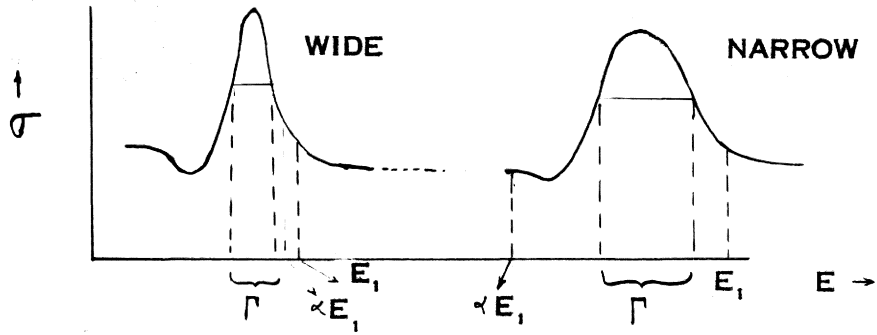


FIG. - 14. PICTORIAL CONCEPT OF NARROW RESONANCE

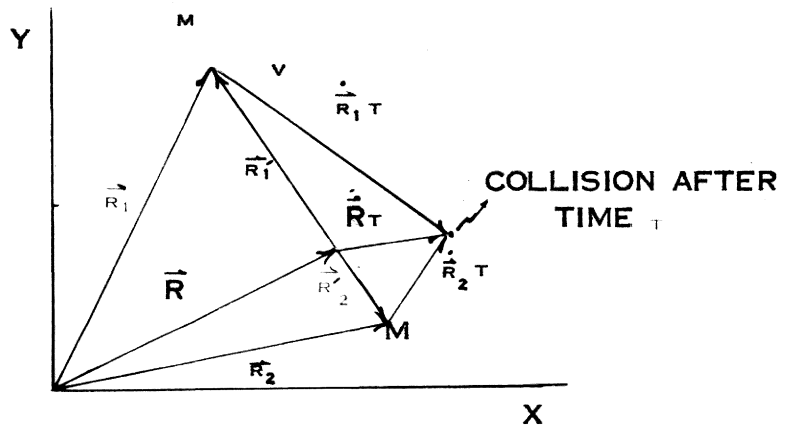


FIG. - 15. POSITION VECTORS

From the point of view of resonance widths peak 8 is wider than peak 1. Continuing, we have

$$\alpha = \left(\frac{A-1}{A+1} \right)^2 = \left(\frac{231}{233} \right)^2 = .983$$

and $(\Delta E_1)_{\max} = (1-.983)21.84 \text{ ev.} = .37 \text{ ev.},$

$$(\Delta E_2)_{\max} = (1-.983)(170.8 \text{ ev.}) = 2.9 \text{ ev.}$$

Since .036 ev. \ll .37 ev. and since .106 \ll 2.9 ev. we conclude by our criteria that both resonances are narrow as is the case for all of the thorium resonances included in table 2. However

$$\frac{\Gamma}{\Delta E_{\max}} = \frac{36}{370} = .0973 \quad \text{and} \quad \frac{106.0}{2900} = .0366$$

which means that peak 8 satisfies narrowness more strongly than peak 1 yet $\Gamma_8 > \Gamma_1$. This, of course, occurs because E_0 for peak 8 is so much larger than E_0 for peak 1. If a neutron appears with energy $E_1 > E_0$ and scatters from thorium it has a greater chance of reducing its energy to below E_0 for peak 8 than for peak 1 and therefore less chance for suffering a second or third collision in thorium assuming that scattering occurs rather than capture in each case.

The low lying 6.7 ev. peak of U^{238} has $\Gamma = 26.5$ mv.
and $\alpha = .9833$.

$$E_1 \approx E_0 = 6.7 \text{ ev. then } (\Delta E)_{\max} = (.0167)6.7 \\ = .1119$$

and

$$\frac{\Gamma}{\Delta E_{\max}} = .207.$$

This peak is much wider than either of the thorium peaks. In all three cases the addition of the Doppler-broadening will weaken the narrowness criterion; this brings the lowest lying peaks out of the narrow classification.

Analytic evaluation of the resonance integral is more easily obtained for the narrower resonances of the higher energy region, and thorium should prove easier than uranium in this respect. See reference (19) for additional details.

Presumably we can arrive at an estimate of REP_{∞}^U by calculating the value of the resonance integral for each of the eight peaks and adding them to get an effective resonance integral I. Then

$$REP_{\infty}^U = \exp \left\{ - \frac{I_{nTh}}{\xi \Sigma_p} \right\} .$$

The calculations leading to the values in table 10 are based on the curves of figure 3-3 of reference (5) and equation (31-3) of the same reference.

$$I = \sigma_p \frac{\Gamma_x}{E_0} \int_0^{\infty} \frac{\psi(x, \theta)}{\psi(x, \theta) + \beta} dx \quad (6.11)$$

We will now present a calculation for the REP' based on the analytical expressions valid for the narrow resonance approximation in homogeneous mixtures. The following equations will be employed where REP' is replaced by P:

$$P = e^{-\left\{ \sum_{i=1}^8 I_i \frac{n_{Th}}{\sum_p} \right\}} \quad (6.12)$$

$$I_i = \frac{\sigma_p \Gamma_x}{E_0} J_i(\theta, \beta) \quad (6.13)$$

$$J_i(\theta, \beta) = \int_0^{\infty} \frac{\psi(x, \theta_i)}{\psi(x, \theta_i) + \beta_i} dx \quad (6.14)$$

$$\xi = \sum_{i=1}^4 \xi_i c_i, \quad c_i = \frac{\sum s_i}{\sum_{i=1}^4 \sum s_i} \quad (6.15) \quad (6.16)$$

$$\sigma_p = \frac{\sum_p}{n_{Th}} \quad (6.17)$$

TABLE. 10

SAMPLE DATA AND RESULTS FOR AN ANALYTICAL CALCULATION WITH $N_{TH} = .9013 \times 10^{21}$ ATOMS CM^3									
PEAK NUMBER	E_0 IN E.V.	Γ_r IN M V	$\theta = \frac{1}{\sqrt{t}}$	$\frac{\sigma_p \Gamma_r}{E_0}$ IN BARNs	$\beta = \frac{\sigma_p}{\sigma_0}$	$j(\beta)$	$J(\theta, \beta)$ CM^{-1}	$I_i(\theta, \beta)$ IN BARNs	$\sigma_0 = \frac{\Gamma_r}{\Gamma} \sigma_r$ BARNs
1	21.84	34	.3691	2.344	.2058	14.33	4.9	11.49	7316
2	23.48	39	.4252	2.501	.1366	13.74	5.1	12.76	11026
3	59.55	21	.1615	.531	.1950	14.25	6.0	3.19	7720
4	69.20	43	.4725	.934	.0842	16.36	7.0	6.54	17887
5	113.15	42	.2388	.559	.3157	14.95	3.5	1.96	4770
6	121.00	41	.2614	.510	.2250	14.46	4.6	2.35	6690
7	129.40	41	.1854	.471	1.0649	16.70	1.3	.61	1414
8	170.80	48	.3887	.423	.1808	14.14	4.9	2.07	8325

FOR THIS TABLE $\sigma_p = 1505$ BNS, $J = .875$, $\sum p = 1.3572 \text{ cm}^{-1}$ AND
 $REP_0 = .9689$.

$$\sum_p = n_{Th} \sigma_{pa} + \sum_{NoH} \quad (6.18)$$

$$\beta = \frac{\sigma_p}{\sigma_o} \quad (6.19)$$

$$\sigma_o = \frac{4\pi}{k^2} \frac{\Gamma_n}{\Gamma} = \frac{2.6 \times 10^6}{E_o} \frac{\Gamma_n}{\Gamma} = \frac{\Gamma}{\Gamma_n} \sigma_{os} \quad (6.20)$$

$$\xi_i = 1 + \frac{\alpha_i \ln \alpha_i}{1 - \alpha_i} \quad (\text{See pp. 81-83 of reference 12}) \quad (6.2.)$$

$$\xi_i \approx \frac{2}{A_i + 2/3} \quad \text{for } A_i > 10 \quad (6.22)$$

where σ_{pa} is the potential scattering cross section of the absorber which is thorium. These equations and the necessary data are found in reference (5). Reference is also made to tables 1 and 2 for the necessary peak parameters. Assuming $n_{Th} = .6231 \times 10^{21}$ atoms/cm³ we have

$$\sum_{NoH} = 1.41 \text{ cm}^{-1}$$

$$\begin{aligned} \sum_p &= n_{Th} \sigma_{pa} + \sum_{NoH} \\ &= (.6231 \times 10^{21}) 10.5 \times 10^{-24} \text{ cm}^{-1} + 1.4114 \text{ cm}^{-1} \\ &= 1.418 \text{ cm}^{-1}. \end{aligned}$$

$$\bar{f} = \frac{f_{Th} \sum_{Th} + f_o \sum_o + f_N \sum_N + f_H \sum_H}{1.418}$$

$$f_{Th} \approx \frac{2}{232.67} = .0086$$

$$f_o \approx \frac{2}{16.67} = .1200$$

$$f_N \approx \frac{2}{14.67} = .1363$$

$$f_H = 1$$

$$\sum_o = (38.91 \times 10^{21})(3.8 \times 10^{-24}) = .14786 \text{ cm}^{-1}$$

$$\sum_N = 2.492(9.1) \times 10^{-3} = .02268 \text{ cm}^{-1}$$

$$\sum_H = (61.43)(20.2) \times 10^{-3} = 1.24089 \text{ cm}^{-1}$$

$$\bar{f} = \frac{(.0086)(.0665) + (.12)(.148) + (.136)(.0227) + (1.241)}{1.418} =$$

.890

$$\sigma_p = 10.5 \text{ bns} + \frac{1.411}{.6231} \times 10^3 \text{ bns} = 2270.3 \text{ bns}$$

$$\beta = \frac{\sigma_p}{\sigma_o} .$$

To proceed with the calculation we refer to figure 3-3 and table 3-3 of reference 5⁽¹⁾, where $J(\theta, \beta)$ is given as a function of j .

$$\beta = 2^j \times 10^5 \quad \text{so that}$$
$$j = \frac{5 + \log \beta}{\log 2} .$$

Table 10 gives the data and resonance integral values from each peak for $n_{\text{Th}} = .9013 \times 10^{21} \text{ atom/cm}^3$. Proceeding for $n_{\text{Th}} = .6231 \times 10^{21} \text{ atoms/cm}^3$ we obtain

$$\sum_{i=1}^8 I_i = 35.34 \text{ bns.}$$

The separate I_i 's are obtained from equation (6.13). Finally, applying equation (6.12) we obtain $P = .9827$ which is 0.5% higher than the value calculated by the Monte Carlo.

It should be noted in table 10 that over one half of the total absorption contribution comes from the first

(1) The same figure and table appear in volume 1 of Nuclear Science and Engineering p. 74 and 76 (1956) where the figure is larger.

two peaks. Peak 4 is the largest in magnitude including the Doppler peak reduction and yet does not contribute as much as either 1 or 2. This means that peak 4 is narrower than peaks 1 and 2 by our criteria. Similarly for peak 6. It is interesting to note that the first peak of uranium (6.7 ev.) contributes over 78% of the absorption. This means that it must not only be large in magnitude but very wide by our criteria.

Table 11 gives the comparison between Monte Carlo and analytical calculations.

We now refer to figure 3 on page 78 of the reference listed in footnote (1) where the effective integral for Th^{232} is given as a function of σ_p . In the range of σ_p from 400 bns. to 2000 bns. there are two measurements that fall somewhat below the theoretical resonance integral values for 300 °K. The first two entries of table 12 have σ_p in the same range and the corresponding effective resonance integral falls below the experimental points. Several explanations of these differences are as follows:

1. Table 12 lists I_{eff} calculated by Dresner's method but using only the lowest eight resonances while Dresner used fifteen taken from Hughes and Harvey (8).
2. Several parameters (particularly σ_0) that Dresner used are in doubt. The σ_0 reported in reference (5) is too large in several cases.

TABLE. 11

COMPARISON OF MONTE CARLO AND ANALYTICAL VALUES FOR REP _∞									
N_{TH} $\times 10^{21}$ CM^{-3}	REP BY MONTE CARLO	$\frac{N_{TH}}{\sum_p} \left(\sum_{i=1}^8 I_i \right)$	NR $e^{-\frac{N_{TH}}{\sum_p} \left(\sum_{i=1}^8 I_i \right)}$	\bar{f}	\sum_p	% DIFFER- ENCE COLUMNS 2 AND 4	NR $1 - \frac{N_{TH}}{\sum_p} \left(\sum_{i=1}^8 I_i \right)$	% DIFFER- ENCE COLUMNS 2 AND 8	ρ
.2439	.9893	.01345	.9865	.912	1.459	.28	.9865	.28	5981.4
.3991	.9814	.01805	.9838	.904	1.447	.24	.9837	.23	3625.9
.6231	.9778	.02471	.9827	.890	1.418	0.50	.9826	.49	2270.3
.9013	.9649	.03349	.9694	.875	1.357	0.46	.9689	.41	1505.9
1.5381	.9458	.05143	.9569	.825	1.161	1.16	.9560	1.07	754.9

TABLE. 12.

EFFECTIVE RESONANCE INTEGRALS

$N_{TH} \times 10^{21}$ ATOMS/CM ³	σ_p IN BARNs	I_{EFF} IN BARNs
1.5891	754.9	27.41
.9013	1505.9	40.95
.6231	2270.3	35.34
.3991	3625.9	53.56
.2439	5981.4	73.37

3. Dresner's calculations indicate that the unresolved resonances may contribute as much as 30% of the total value of the effective resonance integral. If 30% is added to the high concentration value in table 12, I_{eff} falls in line with the measured value. For higher concentrations, larger percentages due to the unresolved resonances are expected because of self shielding of the resolved resonances.

It appears that Dresner's theoretical calculations are too high because the data he uses (8) give values of σ_0 and Γ_n that are too large. The data used in this paper comes from Bollinger and Cote' (1) and Rosen (18). It is believed that these sources of the resonance parameters for thorium are more reliable with the latter being the most recent.

6.6 Conclusions

The Monte Carlo calculation gives the following contributions to the resonance escape problem:

1. It indicates the geometric effect on the resonance escape probability allowing calculations for finite and rather small reactors.

2. It gives the relative contributions of thorium absorption and geometric leakage as a function of concentration.

3. It provides an analog calculation of the thorium resonance escape probability independent of the theoretical assumptions leading to equation (6.12).

4. If this Monte Carlo program were translated from IBM-650 language to the IBM-704 language the whole problem could be run in less than two hours. On the IBM-650 it takes about 65 hours.

CHAPTER 7.

SUGGESTED EXTENSIONS

A series of radial (off the beam axis) distributions for sixteen values of z (the coordinate along the beam axis) have been determined by least squares fitting with a function of the form

$$f(r,z) = a(z)r^{b(z)}e^{-c(z)r} \quad (7.1)$$

to the position distributions obtained from the water moderated Monte Carlo which was used as the source for the REP Monte Carlo (21). These distributions coupled with the uniformly distributed "first arrival" energies and the assumption of an isotropically directed set of "first arrival" initial velocity vectors may well provide a sufficient basis for Monte Carlo sampling to initiate a history. This would replace the card-read source routine used in this paper. It may well happen that the programming of this new source routine may overtax the storage of a "bare" IBM-650 in which case a larger computer would be necessary. Since "reading" is very slow, we might anticipate an overall speed up of the computations allowing more statistics in a shorter running time. This would

help remove the large statistical fluctuations implied in the results for such quantities as P_{ab}' .

It should prove interesting to modify the program to provide a check for Safanov's water-uranium curve (19).

A larger computer would provide more storage to allow more definitive tabular histograms with which to approximate the resonance cross sections.

When data with better resolution becomes available the higher energy resonances could be included with more precision. All that need be done to the program is to increase the number of energy gaps tested and expand the number of Ψ and χ tables correspondingly. The basic structure of the program would thus be unaltered. This refinement will not likely improve the results significantly.

With a faster computer one could examine the effects of temperature variation on the REP. This can be done by using different Doppler widths which provide the source of temperature dependence of REP.

ACKNOWLEDGMENTS

I wish to thank Dr. Wilbur Payne for the initial ideas to this research and for his consultation during its progress.

My thanks go also to Dr. D. Willard who ably advised me during the major portion of the project.

I am indebted to Mr. _____ for providing valuable data by altering his Monte Carlo program for water moderation.

Dr. R. E. Bargmann gave valuable help with programming and statistical analysis.

Others who have contributed time and energy are Mrs. _____ with the IBM equipment, Mr. _____ for tabulating services, Mr. _____ for the lettering of tables and figures and Mrs. _____ for her masterful typing of the manuscript.

A special note of thanks goes to my wife, _____, who has known not a few sacrifices throughout the pursuit of this goal.

The research presented in this paper was sponsored by the United States Atomic Energy Commission.

BIBLIOGRAPHY

Literature Cited

1. Bollinger, L. M. and Cote'c R. E., "Thorium Resonance Data", Argonne National Laboratory, 1956, Private Communication.
2. Cashwell, E. D. and Everett, C. J., "A Practical Manual on the Monte Carlo Method for Random Walk Processes", Pergamon Press, pp. 4-10, (1959).
3. *ibid*, pp. 27-29.
4. *ibid*, pp. 128-133.
5. Dresner, L., Resonance Absorption in Nuclear Reactors, Pergamon Press, pp. 6-37, (1960).
6. *ibid*, pp. 115-123.
7. Glasstone, S., and Edlund, M., The Elements of Nuclear Reactor Theory, pp. 136-168, Van Nostrand (1952).
8. Hughes, D. J. and Harvey, J. A., BNL-325 Second Edition (1958).
9. Kahn, Herman, "Application of Monte Carlo", Rand Corporation, AECU-3259, pp. 3-19, 83-88 (1954).
10. Kahn, Herman, "Random Sampling Techniques in Neutron Attenuation Problems - I", *Nucleonics*, Volume 6, pp. 27-33, (1950).

11. Hughes, D. J., and Egger, C., Resonance Absorption of Thorium, CP 3093, July (1945).
12. Meghreblian, R. V., and Holmes, D. K., Reactor Analysis, McGraw-Hill, (1960).
13. Morton, K. W., "A Calculation of Resonance Escape Probability by Monte Carlo Methods", Second International Conference on the Peaceful Uses of Atomic Energy, A/CONF.15/P/19 United Kingdom, 21 May 1958.
14. Neumann, H., "Resonance Escape Probability in Reactor Lattices", Proceedings of the Brookhaven Conference on Resonance Absorption of Neutrons in Nuclear Reactors, pp. 110-115 (1956).
15. Richtmyer, R. D., "Resonance Capture Calculations for Lattices by the Monte Carlo Method", Proceedings of the Brookhaven Conference on Resonance Absorption of Neutrons in Nuclear Reactors, pp. 82-89 (1956).
16. Richtmyer, R. D., Van Norton, R., Wolfe A., "The Monte Carlo Calculation of Resonance Capture in Reactor Lattices", Second United Nations International Conference on the Peaceful Uses of Atomic Energy, A/CONF.15/P/2489, USA, 8 August 1958.
17. Rose, M. E., et. al., "A Table of the Integral $\Psi(x,t)$ ", AEC WAPD-SR-506, Vol. II, Oct. (1954).

18. Rosen, J., Thorium Level Parameters, Columbia Nevis Cyclotron Laboratory, Private Communication, Sept. (1960).
19. Safanov, G., "Resonance Escape Probability in Natural Uranium and Light and Heavy Water Mixtures", Rand Corporation, Proceedings of the Brookhaven Conference on Resonance Absorption of Neutrons in Nuclear Reactors, pp. 79-81 (1956).
20. Sampson, J. B., and Chernick, J., Resonance Escape Probability in Thermal Reactors, Progress in Nuclear Energy, Series I, Physics and Mathematics Volume II, Pergamon Press, pp. 223-270 (1958).
21. Settles, R., M. S. Thesis, Virginia Polytechnic Institute, (1961).
22. Spinney, K. T., "Resonance Absorption in Homogeneous Mixtures", Proceedings of the Brookhaven Conference on Resonance Absorption of Neutrons in Nuclear Reactors, BNL 433 (C-24) (1956).

Literature Examined

1. Egelstaff, P. A. and Hughes, D. J. "Resonance Structure of U^{233} , U^{235} and Pu^{239} ", Progress in Nuclear Energy, Series I, Physics and Mathematics, Volume 1, McGraw-Hill, pp. 55-68 (1956).
2. Goertzel, G. and Kalos, M. H., "Monte Carlo Methods in Transport Problems", Progress in Nuclear Energy, Series I, Physics and Mathematics, Volume II, McGraw-Hill, pp. 315-369 (1958).
3. Dresner, L., "The Effective Resonance Integrals of U-238 and Th-232", Nuclear Science and Engineering, Volume 1 (1956).
4. Meyer, H. A., Symposium on Monte Carlo Methods, pp. 146-190, an article by Kahn, H., pp. 249-264, an article by Butler, J. W., John Wiley and Sons (1954).
5. Harvey, J. A. and Schwartz, R. B., "Thermal and Resonance Neutron Cross Sections of Heavy Nuclei", Progress in Nuclear Energy, Series I, Physics and Mathematics, Volume II, pp. 51-90 (1958).
6. Spanier, J., "Monte Carlo Methods and Their Application to Neutron Transport Problems", Bettis Atomic Power Laboratory, Pittsburgh, Pa., WAPD 195: A wealth of material with mathematical rigor (1959).

7. Spanier, J., Kuehn, H., Gullinger, W., "Tut-15 - A Two Dimensional Monte Carlo Calculation of Capture Probabilities for the IBM-704", Bettis Atomic Power Laboratory, Pittsburgh, Pa., WAPD-TM-125, Nov. (1959).

**The vita has been removed from
the scanned document**

APPENDIX I

The Fundamental Theorem of Monte Carlo

The primary question to be answered in a Monte Carlo problem is how to select the value of a variable from many possible values where the possibilities are described by a frequency function or probability density function. The answer to that question is provided by the following theorem. Theorem: Given a random number N_r uniformly distributed on the interval $(0,1]$ and a real, positive, single valued, continuous function $f(x)$ defined on the interval - x such that

$$\int_{-\infty}^{\infty} f(x)dx = 1 .$$

Then for $N_r = \int_0^X f(x)dx$ we have that X is a random

variable with frequency function $f(x)$.

Proof: The indefinite integral

$$F(x) = \int_{-\infty}^x f(x')dx' \quad \text{exists} \quad (1)$$

because of the given conditions on $f(x)$.

$$\lim_{x \rightarrow \infty} F(x) = \int_{-\infty}^{\infty} f(x')dx' = 1$$

$$\lim_{x \rightarrow -\infty} F(x) = \int_{-\infty}^{-\infty} f(x')dx' = 0 .$$

$F(x_1) < F(x_2)$ for $x_1 < x_2$ since $f(x) > 0$ for all x .

We then recognize $F(x)$ as a monotonically increasing function so

$$F_{\max} = F(\infty) = 1$$

and

$$F_{\min} = F(-\infty) = 0$$

$$0 < F(x) \leq 1 .$$

From equation (1) and the fundamental theorem of integral calculus

$$\frac{dF}{dx} = f(x), \quad \text{or} \quad dF = f(x)dx . \quad (2)$$

This is of the form $g(F)dF = f(x)dx$ where $g(F) = 1$. We thus say that $f(x)$ in (x, f) space maps into $g(F)$ in (F, g) space. Since $g(F) = 1$, F is uniformly distributed in (F, g) space on $(0, 1]$. F then satisfies the conditions for being N_r and we can write $F(x) = N_r$ or $x = F^{-1}(N_r)$. Since a function of a random variable is also a random variable we conclude that x is a random variable and by (2) its frequency function is $f(x)$.

$F(x)$ is called the distribution function of x and gives the probability that $x' < x$, i.e.,

$$F(x) = P(x' < x) = \int_{-\infty}^x f(x')dx' .$$

APPENDIX II

1. Cross Section Formulas*

In the present paper the neutron energies for all collisions is so low that only interactions for $l = 0$ occur.

The cross sections for absorption and scattering in terms of l are given by

$$\sigma_{ab,1} = \frac{\pi}{k^2} \sum_1 (2l+1) (1 - |\eta_l|^2) \quad (1)$$

$$\sigma_{sc,1} = \frac{\pi}{k^2} \sum_1 (2l+1) |1 - \eta_l|^2 \quad (2)$$

where k = the neutron wave number in the center of mass

$$= \sqrt{\frac{2\mu E}{\hbar^2}}$$

and l = the orbital angular momentum quantum number.

η_l is a factor giving the phase shift and amplitude change in the scattered partial wave.

For $l = 0$ the equations (1) and (2) become

* The equations (1) to (12) are derived in the book, "Theoretical Nuclear Physics" by Blatt and Weisskopf.

$$\sigma_{ab,o} = \frac{\pi}{k^2} (1 - |\eta_o|)^2 \quad (3)$$

$$\sigma_{sc,o} = \frac{\pi}{k^2} |1 - \eta_o|^2 \quad (4)$$

Introduction of the quantity

$$f_o = R \left(\frac{dU_o}{dr} \frac{1}{U_o} \right)_{r=R} \quad (5)$$

where U_o is the radial wave function for $l = 0$ and R is the nuclear radius gives

$$\sigma_{ab,o} = \frac{\pi}{k^2} \frac{-4(\text{Im}f_o)kR}{(\text{Re}f_o)^2 + (\text{Im}f_o - kR)^2} \quad (6)$$

$$\sigma_{sc,o} = \frac{\pi}{k^2} |A_{\text{pot}} + A_{\text{res}}|^2 \quad (7)$$

where $A_{\text{pot}} = e^{i2kR} - 1$ (8)

$$A_{\text{res}} = \frac{-2ikR}{f_o - ikR} \quad (9)$$

With the introduction of resonance level widths Γ_n, Γ_γ
and Γ

where Γ_n = neutron level width

Γ_γ = radiative capture level width

$$\Gamma = \Gamma_n + \Gamma_\gamma \quad (10)$$

we obtain with suitable approximations and algebraic manipulations

$$\sigma_{ab,o} = \frac{\pi}{k^2} \frac{\Gamma_\gamma \Gamma_n}{(E - E_o)^2 + \frac{\Gamma^2}{4}} \quad (11)$$

$$\sigma_{sc,o} = \frac{\pi}{k^2} \frac{\Gamma_n^2}{(E - E_o)^2 + \frac{\Gamma^2}{4}} + \frac{4\pi R}{k} \frac{n(E - E_o)}{(E - E_o)^2 + \frac{\Gamma^2}{4}} + 4\pi R^2 \quad (12)$$

E and E_o are the center of mass neutron energies "off resonance" and "on resonance" respectively. Equations (11) and (12) are the single level Breit-Wigner formulas for an $l=0$, $I=0$ interaction. The nuclear spin I is zero for thorium.

2. The Doppler Broadening Effect

We wish to include in our description of the resonance cross sections the effect of the motion of the target nuclei. To do this we use a relative energy formulation.

Define $E_{\text{relative}} \equiv E_{\text{center of mass}} \equiv E'$

then $E' = \frac{1}{2}\mu\dot{\mathbf{r}}^2$ where $\mu = \frac{mM}{m+M}$

m = neutron mass

M = target nucleus mass

$\dot{\mathbf{r}}$ = relative velocity

$\dot{\mathbf{r}} = \dot{\mathbf{r}}_1 - \dot{\mathbf{r}}_2$ (see figure 15)

$$E' = \frac{1}{2}\mu\dot{\mathbf{r}}^2$$

$$= \frac{1}{2}\mu(\dot{\mathbf{r}}_1 - \dot{\mathbf{r}}_2)^2 .$$

Let $\dot{\mathbf{r}}_1 = \hat{\nu}v$ then we have

$$E' = \frac{1}{2}\mu(v^2 - 2\hat{\nu}\cdot v\dot{\mathbf{r}}_2 + \dot{\mathbf{r}}_2^2) = \mu v^2 \left(\frac{1}{2} - \frac{\hat{\nu}\cdot\dot{\mathbf{r}}_2}{v} + \frac{1}{2}\frac{\dot{\mathbf{r}}_2^2}{v^2} \right)$$

now for $v \gg |\dot{\mathbf{r}}_2|$

$$E' \simeq \mu v^2 \left(\frac{1}{2} - \hat{\nu}\cdot\frac{\dot{\mathbf{r}}_2}{v} \right) \quad \text{but } \hat{\nu}\cdot\frac{\dot{\mathbf{r}}_2}{v} = U_x$$

where U_x is the component of the target atom velocity in the $\hat{\nu}$ direction. This becomes

$$E' \simeq \frac{1}{2}\mu v^2 \left(1 - \frac{2U_x}{v} \right) . \tag{1}$$

We define $E'_0 \equiv \frac{1}{2}\mu v^2$ called the relative energy of m and M for M at rest.

Then $v = \sqrt{\frac{2E'_0}{\mu}}$ and $\mu v = \sqrt{2\mu E'_0}$

so that equation (1) becomes

$$\underline{\underline{E' \simeq E'_0 - \sqrt{2\mu E'_0} U_x}} \quad (2)$$

$$\text{and } dE' = -\sqrt{2\mu E'_0} dU_x \quad (3)$$

If we assume the speeds of the target atoms to have a Maxwellian distribution and that the system contains isotropic motion (no direction preferred) only, we can write the one dimensional distribution for U_x by the expression

$$f(U_x)dU_x = \sqrt{\frac{M}{2\pi kT}} e^{-\frac{M}{2kT} U_x^2} dU_x \quad (4)$$

but $f(U_x)dU_x = f(E')dE'$.

Therefore substituting equations (2) and (3) into equation (4) we have

$$f(E')dE' = \sqrt{\frac{M}{4\pi\mu\tau E'_0}} e^{-\frac{M}{4\mu\tau E'_0} (E'_0 - E')^2} dE' \quad (5)$$

where $\tau = kT$.

We now wish to use this distribution to calculate an effective cross section. The function $f(E')$ is actually a probability density function since it has been normalized ($\int_0^{\infty} f(E') dE' = 1$)

therefore
$$\sigma_{(E'_0, T)} = \int_0^{\infty} \sigma(E') f(E') dE' . \quad (6)$$

$$\sigma_{\text{Total}, l} = \sigma_{\text{ab}, l} + \sigma_{\text{sc}, l} \quad \text{and for } l = 0$$

which is our case, since the neutron energies are too small to have larger angular momenta, we would have

$$\sigma_{T, 0} = \sigma_{\text{ab}, 0} + \sigma_{\text{sc}, 0} .$$

For future ease of writing we will drop the zero getting the form

$$\sigma_T = \sigma_{\text{ab}} + \sigma_{\text{sc}} \quad (7)$$

which is more explicitly given by the Breit-Wigner equation as

$$\sigma_T = g(s) \frac{\pi}{k^2} \frac{\Gamma_n \Gamma_{\sigma}}{(E-E_0)^2 + \frac{\Gamma^2}{4}} + g(s) \frac{\pi}{k^2} \left| \frac{i \Gamma_n}{(E-E_0) + i \frac{\Gamma}{2}} + e^{2ikR} - 1 \right|^2 + (1-g(s)) 4\pi R^2 \quad (8)$$

where $g(s) = \frac{2s+1}{2(2I+1)}$, $s = I+\frac{1}{2}, I-\frac{1}{2}$ (9)

but for thorium ($I=0$) $g(s) = \frac{2}{2} = 1$

so equation (8) becomes

$$\sigma_T = \frac{\pi}{k^2} \frac{\Gamma_n \Gamma_r}{(E-E_0)^2 + \frac{\Gamma^2}{4}} + \frac{\pi}{k^2} \left| \frac{i\Gamma_n}{(E-E_0) + i\frac{\Gamma}{2}} + e^{2ikR-1} \right|^2 \quad (10)$$

Expanding the second term gives

$$\begin{aligned} \sigma_T = \frac{\pi}{k^2} \frac{\Gamma_n \Gamma_r}{(E-E_0)^2 + \frac{\Gamma^2}{4}} + \frac{\pi}{k^2} \frac{\Gamma_n^2}{(E-E_0)^2 + \frac{\Gamma^2}{4}} + \frac{4\pi R}{k} \frac{\Gamma_n(E-E_0)}{(E-E_0)^2 + \frac{\Gamma^2}{4}} \\ + 4\pi R^2 \end{aligned} \quad (11)$$

where the first term is σ_{ab} and the sum of the rest is σ_{sc} .

$$\text{Let } \sigma_{ab, \max.} = \sigma_{or}, \quad \sigma_{sc, \max} - 4\pi R^2 = \sigma_{os} \quad (12) \quad (13)$$

$$\text{and } \sigma_{pot} = 4\pi R^2. \quad (14)$$

Since the neutron width is proportional to E' with the reduced width being the proportionality constant we have

$$\frac{\Gamma_n}{\sigma_n} = \frac{\sqrt{E'} \Gamma_n^0}{\sqrt{E_0} \Gamma_n} \quad (15)$$

where Γ_n^0 = reduced width

$$o\Gamma_n = \Gamma_n \text{ at resonance.}$$

$$\text{Then } \sigma_{or} = \frac{4\pi}{k_o^2} \frac{o\Gamma_n \Gamma_n}{\Gamma^2} \text{ and } \sigma_{os} = \frac{4\pi}{k_o^2} \left(\frac{o\Gamma_n}{\Gamma} \right)^2. \quad (16) \quad (17)$$

We can now rewrite equation (6).

$$\begin{aligned} \sigma_{(E'_o, t)} &= \int_0^\infty \sigma_T(E') f(E') dE' = \int_0^\infty \sigma_{ab}(E') f(E') dE' \\ &+ \int_0^\infty \sigma_{sc}(E') f(E') dE'. \quad (18) \end{aligned}$$

We proceed to reduce the first term by use of equations (11) to (17).

$$\sigma_{ab}(E'_o, T) = \frac{\sigma_{or}}{\sqrt{\pi}} \int_0^\infty \frac{k_o^2}{k^2} \sqrt{\frac{E'}{E_o}} \frac{e^{-(E'_o - E')^2 / 4\mu\tau E'_o}}{2\sqrt{\mu\tau E'_o} \left(\frac{(E' - E_o)^2}{\Gamma^2/4} + 1 \right)} dE'. \quad (19)$$

We can use the expressions in energy for the k's as follows

$$\frac{k_o^2}{k^2} = \frac{2E_o\mu/h^2}{2E'\mu/h^2} = \frac{E_o}{E'}$$

It is convenient here to introduce the following definitions

$$x = \frac{E'_0 - E_0}{\Gamma/2}, \quad y = \frac{E' - E_0}{\Gamma/2}, \quad \Delta = 2\sqrt{\frac{\mu}{M} \Gamma E'_0} \quad (20) \quad (21) \quad (22)$$

where E_0 is the energy at resonance

$$\theta \equiv \Gamma / \Delta \quad \text{and} \quad dy = \frac{2}{\Gamma} dE' \quad (23) \quad (24)$$

In equation (19) $2\sqrt{\frac{\mu}{M} \Gamma E'_0} \simeq 2\sqrt{\frac{\mu}{M} \Gamma E_0}$

for $|E'_0 - E_0| \ll E_0$ and so equation (19) becomes

$$\sigma_{ab}(E'_0, T) \simeq \frac{\sigma_{or}}{\sqrt{\pi}} \int_{-E_0/\Gamma/2}^{\infty} \sqrt{\frac{E_0}{E'}} \frac{e^{-\frac{\theta^2}{4}(x-y)^2} \Gamma/2 dy}{(y^2+1)}$$

$$\sigma_{ab}(E'_0, T) = \sigma_{or} \frac{\theta}{2\sqrt{\pi}} \int_{-\infty}^{\infty} \sqrt{\frac{E_0}{E'}} \frac{e^{-\frac{\theta^2}{4}(x-y)^2}}{1+y^2} dy, \quad E_0 \gg \Gamma. \quad (25)$$

For $|y| \gg |x|$ the integrand is very small and if one stays away from the pole at $E'=0$ the only contributions that are significant come for $E' \simeq E'_0$. Another way of saying this is that the function $\sqrt{E_0/E'}$ is very slowly

varying compared to $\frac{e^{-\frac{\theta^2}{4}(x-y)^2}}{1+y^2}$ which drives the integrand

to zero long before a noticeable change in $\sqrt{E_0/E'}$ can occur. This allows us to write

$$\sigma_{ab}(E', T) = \sqrt{\frac{E_0}{E'}} \sigma_{or} \psi(x, \theta) \quad (26)$$

$$\text{where } \psi(x, \theta) = \frac{\theta}{2\sqrt{\pi}} \int_{-\infty}^{\infty} \frac{e^{-\frac{\theta^2}{4}(x-y)^2}}{1+y^2} dy. \quad (27)$$

We now reduce the second term of equation (18) using equations (11) to (17) and (5) where (5) can now be given in the form

$$\begin{aligned} f(E')dE' &= f(y)dy = \frac{\theta}{2\sqrt{\pi}} e^{-\frac{\theta^2}{4}(x-y)^2} dy \\ \sigma_{sc}(E'_0, T) &= \frac{\theta \sigma_{os}}{2\sqrt{\pi}} \int_{-\infty}^{\infty} \frac{e^{-\frac{\theta^2}{4}(x-y)^2}}{1+y^2} + \frac{\theta}{2\sqrt{\pi}} \int_{-\infty}^{\infty} \frac{4\pi R}{k} \frac{\Gamma_n(E'-E_0)/\Gamma^2}{1+y^2} e^{-\frac{\theta^2}{4}(x-y)^2} dy \\ &\quad + \sigma_{pot} \\ &= \sigma_{os} \psi(x, \theta) + \sigma_{pot} + \frac{\theta}{2\sqrt{\pi}} \int_{-\infty}^{\infty} (2\pi R) 2\sqrt{\pi} \frac{2}{r} \frac{\Gamma_n}{k} \frac{y}{1+y^2} e^{-\frac{\theta^2}{4}(x-y)^2} dy. \end{aligned}$$

The last term becomes

$$\frac{\theta}{2\sqrt{\pi}} \int_{-\infty}^{\infty} \sqrt{\sigma_{\text{pot}}} \sqrt{\frac{4\pi(\Gamma_n)^2}{k^2(r)^2}} \frac{2y}{1+y^2} e^{-\frac{\theta^2}{4}(x-y)^2} dy$$

$$\frac{\Gamma_n}{k} = \frac{\Gamma_n^{\circ} \sqrt{E'}}{\frac{2E'\mu}{k}} = \frac{\Gamma_n^{\circ}}{\{2\mu\}^{\frac{1}{2}}} \quad \text{and} \quad \frac{o/n}{k_0} = \frac{\Gamma_n^{\circ} \sqrt{E_0}}{\frac{2E_0\mu}{k}} = \frac{k \Gamma_n^{\circ}}{\{2\mu\}^{\frac{1}{2}}}$$

$$\therefore \frac{\Gamma_n}{k} = \frac{o/n}{k_0} .$$

Finally,

$$\sigma_{\text{sc}}(E'_0, T) = \sigma_{\text{os}} \psi(x, \theta) + \sigma_{\text{pot}} + \sqrt{\sigma_{\text{pot}} \sigma_{\text{os}}} \frac{\theta}{2\sqrt{\pi}} \int_{-\infty}^{\infty} \frac{2y e^{-\frac{\theta^2}{4}(x-y)^2}}{1+y^2} dy . \quad (28)$$

By defining

$$\chi(x, \theta) = \frac{\theta}{2\sqrt{\pi}} \int_{-\infty}^{\infty} \frac{2y e^{-\frac{\theta^2}{4}(x-y)^2}}{1+y^2} dy \quad (29)$$

we obtain

$$\sigma_{\text{sc}}(E'_0, T) = \sigma_{\text{os}} \psi(x, \theta) + \sqrt{\sigma_{\text{pot}} \sigma_{\text{os}}} \chi(x, \theta) + \sigma_{\text{pot}} . \quad (30)$$

Since $\sigma_T(E'_0, T) = \sigma_{ab}(E'_0, T) + \sigma_{sc}(E'_0, T)$ (31)

we have

$$\sigma_T(E'_0, T) = \sqrt{\frac{E_0}{E'_0}} \sigma_{or} \psi(x, \theta) + \sigma_{os} \psi(x, \theta) + \sqrt{\sigma_{pot} \sigma_{os}} \chi(x, \theta) + \sigma_{pot} \quad (32)$$

To express this in laboratory energies we recall that

$$E'_0 = \frac{1}{2} \mu v^2 = \frac{M}{m+M} E_1 \quad (33)$$

where E_1 is the neutron energy in the laboratory system.

From equation (22) the Doppler width becomes

$$\Delta \approx 2 \sqrt{\frac{mM}{M(m+M)} \gamma E'_0} \approx 2 \sqrt{\frac{mM}{(m+M)^2} \gamma_0 E_1} ,$$

where ${}_0E_1$ is the neutron energy in the laboratory at resonance.

If we let the neutron mass m be equal to one and the target mass M be the isotopic mass number A , we have

$$\Delta = \sqrt{\frac{4 \gamma_0 E_1}{(1+A) \frac{1+A}{A}}} = \frac{1}{1+\frac{1}{A}} \sqrt{\frac{4 \gamma_0 E_1}{A}} \quad \text{and for } A \gg 1$$

$$\Delta \approx \sqrt{\frac{4 \gamma_0 E_1}{A}} \quad (34)$$

The cross section equations given use center of mass energies. If we wish to use laboratory energies we must multiply each energy including level widths by the factor $\frac{m+M}{m}$ or $\frac{1+A}{A}$ in our case. Since only energy ratios appear in the formulas we can use laboratory energies directly. In computing θ , we use equation (34) with no significant error.

3. Properties of $\Psi(x,t)$ and $\chi(x,t)$: where $t = 1/\theta^2$

$$\Psi(x,t) = \frac{1}{2\sqrt{\pi t}} \int_{-\infty}^{\infty} \frac{e^{-\frac{(x-y)^2}{4t}}}{1+y^2} dy = \frac{\theta}{2\sqrt{\pi}} \int_{-\infty}^{\infty} \frac{e^{-\frac{\theta^2}{4}(x-y)^2}}{1+y^2} dy \quad (1)$$

$$\chi(x,t) = \frac{1}{2\sqrt{\pi t}} \int_{-\infty}^{\infty} \frac{2ye^{-\frac{(x-y)^2}{4t}}}{1+y^2} dy = \frac{\theta}{2\sqrt{\pi}} \int_{-\infty}^{\infty} \frac{2ye^{-\frac{\theta^2}{4}(x-y)^2}}{1+y^2} dy \quad (2)$$

$$\chi(x,t) = 2x\Psi + 4t \frac{\Psi}{x} \quad (3)$$

which can be derived simply by taking the derivative of Ψ with respect to x and re-using (1) and (2).

We wish to obtain asymptotic expressions for Ψ and χ that will afford ease in machine computation for x beyond a value that provides only a small error. For smaller values of x numerical integrations are available in tabular form (16).

The asymptotic solution for $\Psi(x,t)$ can be obtained as follows:

Expand the factor $1/1+y^2$ of the integrand of equations (1) and (2) in a Taylor series about $y = x$ to obtain

$$\begin{aligned} \frac{1}{1+y^2} &= \frac{1}{1+x^2} + (y-x) \left\{ \frac{-2x}{(1+x^2)^2} \right\} + \frac{(y-x)^2}{2} \left\{ -\frac{2}{(1+x^2)^2} + \frac{8x^2}{(1+x^2)^3} \right\} \\ &+ \frac{(y-x)^3}{3} \left\{ \frac{24x}{(1+x^2)^3} - \frac{48x^3}{(1+x^2)^4} \right\} + \frac{(y-x)^4}{4} \left\{ \frac{24}{(1+x^2)^3} - \frac{288x^2}{(1+x^2)^4} \right. \\ &\left. + \frac{384x^4}{(1+x^2)^5} \right\} + \dots \end{aligned} \quad (4)$$

Upon substitution of equation (4) into (1) and (2) we obtain

$$\Psi_{\text{asymptotic}} = \frac{1}{1+x^2} \left[1 + 2t \frac{3x^2-1}{(1+x^2)^2} + \frac{12t^2}{(1+x^2)^4} (1-10x^2+5x^4) + \dots \right] \quad (5)$$

$$\chi_{\text{asymptotic}} = \frac{2x}{1+x^2} \left[1 + \frac{2t(x^2-3)}{(1+x^2)^2} + \frac{12t^2}{(1+x^2)^4} (5-10x^2+x^4) + \dots \right]. \quad (6)$$

In order to neglect the third term in equation (5) we require that

$$2t \frac{3x^2-1}{(1+x^2)^2} \gg \frac{12t^2}{(1+x^2)^4} (1-10x^2+5x^4)$$

which becomes

$$(1+x^2) \frac{3 + 2/x^2 - 1/x^4}{5 - 10/x^2 + 1/x^4} \gg 6t$$

and for large x

$$\frac{3}{5}x^2 \gg 6t \quad \text{or} \quad x^2 \gg 10t .$$

Neglect of the third term in equation (6) by similar reasoning requires $x^2 \gg 6t$.

APPENDIX III

Nuclide Number Densities

We shall define the following symbols:

- c = concentration of reactor solution
 ρ = density of the reactor solution in gm/cm³
 n_{Th} = number of thorium atoms per cm³
 n_{Ox} = number of oxygen atoms per cm³
 n_N = number of nitrogen atoms per cm³
 n_H = number of hydrogen atoms per cm³.

One can show for a $Th(NO_3)_4$ aqueous solution that

$$\begin{aligned}n_{Th} &= 1.255 \times 10^{21} c \\n_N &= 5.020 \times 10^{21} c \\n_{Ox} &= 12n_{Th} + 26.64 \left(\frac{1}{c} - 1 \right) n_{Th} \\n_H &= 53.29 \left(\frac{1}{c} - 1 \right) n_{Th} .\end{aligned}$$

Using the density vs. concentration curve one can, for a specified c , calculate the number densities from the above equations.

APPENDIX IV

The Programs

1. Input and Output Data.

(a) Input Data:

The initial parameters for beginning a neutron history are fed into the IBM-650 by reading punch cards that contain eight 10-digit words. We have the following arrangement of data:

<u>Word</u>	<u>Columns</u>	<u>Quantity</u>	<u>Decimal Point</u>
1	1 - 10	(irrelevant)	-
2	11 - 20	x	4 - 6
3	21 - 30	y	4 - 6
4	31 - 40	z	4 - 6
5	41 - 50	E	8 - 2
6	51 - 60	W	1 - 9
7	61 - 70	e	1 - 9
8	71 - 80	Φ	1 - 9

E is the first energy the neutron has below 1000 ev. and W is its statistical weight at that energy. W is essentially one, but due to the inclusion of very small absorption during the water moderation some neutrons have a weight slightly less than one.

(b) Output Data:

An output card contains the following information concerning the neutron history:

<u>Word</u>	<u>Column</u>	<u>Quantity</u>	<u>Decimal</u>
1	1 - 10	initial weight, W_{in}	1 - 9
2	11 - 20	final weight, W	1 - 9
3	21 - 30	w^2	2 - 8
4	31 - 40	$N=4317$ $\sum_{i=1}^N i W_{in}$	1 - 9
5	41 - 50	N , the total number of collisions per history	6 - 4
6	51 - 60	$N_{H,i}$ the number of hydrogen collisions on the i^{th} card	6 - 4
7	61 - 70	$N_{ox,i}$ the number of oxygen collisions...	6 - 4
8	72 and 73	90 means out 01 means low	
	74 - 80	$N_{Th,i}$ the number of thorium collisions...	8 - 2

2. The Data Extraction Program.

This program adds the words on the output cards to provide the following quantities:

$W_1 = \sum_{i=1}^k W_{1i}$, the sum of weights for neutrons surviving to energies less than 10 ev. where k is the number of histories producing an energy less than 10 ev.

$W_{in} =$ the sum of initial weights from all source cards.

$W_0 =$ the sum of weights that escape from the pile before an energy less than 10 ev. is attained.

$$W_1^2 = \sum_{i=1}^k W_{1i}^2$$

$N = \sum_{i=1}^{K+k} N_{c,i}$ K = number of histories resulting in escape from the pile.

$$N_H = \sum_{i=1}^{K+k} N_{H,i} .$$

$$N_{ox} = \sum_{i=1}^{K+k} N_{ox,i}$$

$$N_{Th} = \sum_{i=1}^{K+k} N_{Th,i} .$$

THE MAIN PROGRAM

<u>Soap Language</u>				<u>Machine Language</u>			
START	RCD	R0001		0300	70	0351	0301
	RAL	R0006		0301	65	0356	0311
	STL	WS		0311	20	0315	0318
	SRD	0004		0318	31	0004	0331
	ALO	SUMWI		0331	15	0334	0339
	STL	SUMWI		0339	20	0334	0337
	LDD	R0005		0337	69	0355	0308
	STD	ETWO		0308	24	0361	0314
	RAU	ZEROP		0314	60	0317	0321
	STU	COLLB		0321	21	0326	0329
	STU	COLHY		0329	21	0434	0387
	STU	COLOX		0387	21	0342	0345
	STU	COLTH		0345	21	0350	0303
	RAU	R0007		0303	60	0357	0411
	EXIT1	LDD	EXIT1	0000	0411	69	0364
STL		SINA1		0364	20	0319	0322
RAU		R0007		0322	60	0357	0461
EXIT2	LDD	EXIT2	0049	0461	69	0414	0049
	STL	COSA1		0414	20	0369	0372
EXIT3	RAU	R0008		0372	60	0358	0313
	LDD	EXIT3	0000	0313	69	0316	0000
	STL	SINC1		0316	20	0371	0324
EXIT4 MEANF	RAU	R0008		0324	60	0358	0363
	LDD	EXIT4	0049	0363	69	0366	0049
	STL	COSB1	MEANF	0366	20	0421	0374
GAP1	RAU	ETWO		0374	60	0361	0365
	SUP	NINTN		0365	11	0368	0323
	BMI	GAP1	PEAK1	0323	46	0376	0327
LOOP	RAU	NTH		0376	60	0429	0333
	MPY	SIG1		0333	19	0336	0306
	SRD	0006		0306	31	0006	0373
LOOP	STL	SIGTH	LOOP	0373	20	0427	0330
	ALO	SINOH		0330	15	0433	0437
	STL	SIG		0437	20	0341	0344
	RAL	ONE		0344	65	0347	0401
	SLT	0002		0401	35	0002	0307
	DVR	SIG		0307	64	0341	0302

	SRD	0002		0302	31	0002	0511
PEAK1	STL	LAMBD . NR		0511	20	0415	0418
	RAU	PEAK		0327	60	0430	0335
	SUP	8003		0335	11	8003	0343
	STU	PEAK		0343	21	0430	0483
	RAU	PEAK		0483	60	0430	0435
	AUP	ONE		0435	10	0347	0451
	STU	PEAK		0451	21	0430	0533
	RAU	ETWO		0533	60	0361	0465
	SUP	TW027		0465	11	0468	0423
PEAK2	BMI	EQU	PEAK2	0423	46	0426	0477
	RAU	PEAK		0477	60	0430	0485
	AUP	ONE		0485	10	0347	0501
	STU	PEAK		0501	21	0430	0583
	RAU	ETWO		0583	60	0361	0515
	SUP	TW08		0515	11	0518	0473
GAP4	BMI	EQU	GAP4	0473	46	0426	0527
	RAU	ETWO		0527	60	0361	0565
	SUP	FIVE2		0565	11	0568	0523
NEG	BMI	NEG	PEAK3	0523	46	0476	0577
	RAU	NTH		0476	60	0429	0633
	MPY	SIG2		0633	19	0436	0406
	SRD	0006		0406	31	0006	0573
PEAK3	STL	SIGTH	LOOP	0573	20	0427	0330
	RAU	PEAK		0577	60	0430	0535
	AUP	ONE		0535	10	0347	0551
	STU	PEAK		0551	21	0430	0683
	RAU	ETWO		0683	60	0361	0615
	SUP	SIX4		0615	11	0618	0623
PEAK4	BMI	EQU	PEAK4	0623	46	0426	0627
	RAU	PEAK		0627	60	0430	0585
	AUP	ONE		0585	10	0347	0601
	STU	PEAK		0601	21	0430	0733
	RAU	ETWO		0733	60	0361	0665
	SUP	SEV6		0665	11	0668	0673
GAP7	BMI	EQU	GAP7	0673	46	0426	0677
	RAU	ETWO		0677	60	0361	0715
	SUP	TEN5		0715	11	0718	0723
EXPON	BMI	EXPON	PEAK5	0723	46	0526	0727
	RAU	ETWO		0526	60	0361	0765
	MPY	ONE11		0765	19	0768	0338
	SLT	0009		0338	35	0009	0309
	SLO	8002		0309	16	8002	0367
	SLO	FIVEB		0367	16	0320	0325
NEXT1	LDD	NEXT1	1600	0325	69	0328	1600
	RAU	8002		0328	60	8002	0487
	MPY	THRE3		0487	19	0340	0310
	SLO	8002		0310	16	8002	0419
	MPY	NTH		0419	19	0429	0400

	RAL	8003		0400	65	8003	0407
	STL	SIGTH	LOOP	0407	20	0427	0330
PEAK5	RAU	PEAK		0727	60	0430	0635
	AUP	ONE		0635	10	0347	0651
	STU	PEAK		0651	21	0430	0783
	RAU	ETWO		0783	60	0361	0815
	SUP	ELEV8		0815	11	0818	0773
PEAK6	BMI	EQU	PEAK6	0773	46	0426	0777
	RAU	PEAK		0777	60	0430	0685
	AUP	ONE		0685	10	0347	0701
	STU	PEAK		0701	21	0430	0833
	RAU	ETWO		0833	60	0361	0865
	SUP	ONE25		0865	11	0868	0823
PEAK7	BMI	EQU	PEAK7	0823	46	0426	0827
	RAU	PEAK		0827	60	0430	0735
	AUP	ONE		0735	10	0347	0751
	STU	PEAK		0751	21	0430	0883
	RAU	ETWO		0883	60	0361	0915
	SUP	ONE40		0915	11	0918	0873
PEAK8	BMI	EQU	PEAK8	0873	46	0426	0877
	RAU	PEAK		0877	60	0430	0785
	AUP	ONE		0785	10	0347	0801
	STU	PEAK		0801	21	0430	0933
	RAU	ETWO		0933	60	0361	0965
	SUP	ONE85		0965	11	0968	0923
GAP13	BMI	EQU	GAP13	0923	46	0426	0927
	RAU	NTH		0927	60	0429	0983
	MPY	ONE32		0983	19	0486	0456
	RAL	8003		0456	65	8003	0413
EQU	STL	SIGTH	LOOP	0413	20	0427	0330
	RAL	ZEROP		0426	65	0317	0471
	LDD	PEAK		0471	69	0430	1033
	TLU	1900		1033	84	1900	0305
VALUE	ALO	VALUE	8002	0305	15	0408	8002
ACT	RAU	0000	ACT	0408	60	0000	0405
STEP	SUP	PEAK	STEP	0405	11	0430	0835
	STU	0181		0835	21	0181	0484
	RAU	STEP		0484	60	0835	0389
	AUP	ONEC		0389	10	0392	0397
	STU	STEP		0397	21	0835	0388
	RAU	PEAK		0388	60	0430	0885
	AUP	ONEB		0885	10	0438	0393
	STU	PEAK		0393	21	0430	1083
	SLT	0004		1083	35	0004	0443
	SUP	FIVE		0443	11	0346	0851
XGAP	NZU	EQU	XGAP	0851	44	0426	0506
	RAU	STEP		0506	60	0835	0439
	SUP	FIVEB		0439	11	0320	0375
	STU	STEP		0375	21	0835	0488

	RAU	ETWO		0488	60	0361	1015
	SUP	0181		1015	11	0181	0935
	MPY	0185		0935	19	0185	0556
	SRD	0003		0556	31	0003	0417
	STL	XDELE		0417	20	0521	0424
	RAM	XDELE		0424	67	0521	0425
	SLO	0182		0425	16	0182	0537
	BMI	TAB2	ASYMP	0537	46	0390	0391
ASYMP	RAU	XDELE		0391	60	0521	0475
	MPY	XDELE		0475	19	0521	0442
	STL	XSQAR		0442	20	0447	0450
	ALO	ONED		0450	15	0403	0457
	SRD	0002		0457	31	0002	1065
	STL	DIV		1065	20	0469	0422
	RAU	XSQAR		0422	60	0447	0901
	MPY	THREE		0901	19	0304	0474
	SLO	ONED		0474	16	0403	0507
	RAU	8002		0507	60	8002	1115
	MPY	0186		1115	19	0186	0606
	SRD	0002		0606	31	0002	1165
	DVR	DIV		1165	64	0469	0480
	SLT	0003		0480	35	0003	0489
	DVR	DIV		0489	64	0469	0530
	ALO	ONEB		0530	15	0438	0493
	SLT	0003		0493	35	0003	0951
	DVR	DIV		0951	64	0469	0580
	SRD	0003		0580	31	0003	0441
	STL	PSI		0441	20	0395	0348
	RAL	XSQAR		0348	65	0447	1001
	SLO	THREB		1001	16	0404	0409
	SLT	0001		0409	35	0001	1215
	DVR	DIV		1215	64	0469	0630
	RAU	8002		0630	60	8002	0539
	MPY	0186		0539	19	0186	0656
	DVR	DIV		0656	64	0469	0680
	ALO	ONEB		0680	15	0438	0543
	RAU	8002		0543	60	8002	1051
	MPY	TWO		1051	19	0454	0524
	RAU	8002		0524	60	8002	1133
	MPY	XDELE		1133	19	0521	0492
	SRD	0001		0492	31	0001	0349
	DVR	DIV		0349	64	0469	0730
	STL	CHI	COMP	0730	20	0985	0538
TAB2	RAU	0182		0390	60	0182	0587
	STU	XMODT		0587	21	0542	0445
	RAU	PEAK		0445	60	0430	1035
	SRT	0006		1035	30	0006	0399
	SLO	8002		0399	16	8002	0557
	SLT	0009		0557	35	0009	0977

	STU	ARG2		0977	21	0332	1085
	RAU	XMODT		1085	60	0542	0497
	SUP	SPLIT		0497	11	0500	0455
	BMI	MIN	POS	0455	46	0458	0459
MIN	RAU	DEL1		0458	60	0561	1265
	STU	DELTA	SCAN	1265	21	0370	0973
POS	RAU	DEL2		0459	60	0312	0467
	STU	DELTA	SCAN	0467	21	0370	0973
SCAN	RAU	XDELE		0973	60	0521	0525
	BMI	DOWN	UP	0525	46	0428	0479
DOWN	RAU	XMODT	DOWN2	0428	60	0542	0547
DOWN2	AUP	XDELE		0547	10	0521	0575
	SUP	DELTA		0575	11	0370	0625
	BMI	TABLE	YET	0625	46	0478	0529
YET	RAU	ARG2		0529	60	0332	0637
	AUP	ONEE		0637	10	0440	0495
	STU	ARG2		0495	21	0332	1135
	RAU	XMODT		1135	60	0542	0597
	SUP	DELTA		0597	11	0370	0675
	STU	XMODT	DOWN2	0675	21	0542	0547
UP	RAU	XMODT	UP2	0479	60	0542	0647
UP2	SUP	XDELE		0647	11	0521	0725
	SUP	DELTA		0725	11	0370	0775
	BMI	TABLE	YET2	0775	46	0478	0579
YET2	RAU	ARG2		0579	60	0332	0687
	AUP	ONEE		0687	10	0440	0545
	STU	ARG2		0545	21	0332	1185
	RAU	XMODT		1185	60	0542	0697
	SUP	DELTA		0697	11	0370	0825
	STU	XMODT	UP2	0825	21	0542	0647
TABLE	RAU	ARG2		0478	60	0332	0737
	AUP	ONEE		0737	10	0440	0595
	STU	ARG2		0595	21	0332	1235
	LDD	8003		1235	69	8003	0592
	TLU	1700		0592	84	1700	0505
	ALO	PEET	8002	0505	15	0508	8002
PEET	RAU	0000	TERSE	0508	60	0000	0555
TERSE	SLT	0003		0555	35	0003	0463
	SRT	0006		0463	30	0006	1027
	STU	PSI		1027	21	0395	0398
	SUP	8003		0398	11	8003	0605
	SLT	0005		0605	35	0005	0517
	STU	CHI		0517	21	0985	0588
	RAU	XDELE		0588	60	0521	0875
	BMI	NEGIT	SHIFT	0875	46	0528	0629
NEGIT	RAU	CHI		0528	60	0985	0589
	MPY	NEG1		0589	19	0642	0362
	STL	CHI	SHIFT	0362	20	0985	0629
SHIFT	RAU	PSI		0629	60	0395	0449

	SLT	0001		0449	35	0001	0655
	STU	PSI	COMP	0655	21	0395	0538
COMP	RAL	0181		0538	65	0181	1285
	SLT	0004		1285	35	0004	0645
	DVR	ETWO		0645	64	0361	0472
	LDD	GOON	0110	0472	69	0925	0110
GOON	SRD	0003		0925	31	0003	1335
	RAU	8002		1335	60	8002	0593
	MPY	0183		0593	19	0183	0504
	RAU	8002		0504	60	8002	0513
	MPY	PSI		0513	19	0395	0416
	SRD	0007		0416	31	0007	1385
	STL	SIGAB		1385	20	0639	0692
	RAU	PSI		0692	60	0395	0499
	MPY	0184		0499	19	0184	0554
	SRD	0003		0554	31	0003	1315
	STL	TEMP		1315	20	0519	0522
	RAU	SPOT		0522	60	0975	0679
	MPY	0184		0679	19	0184	0604
	LDD	AFT	0110	0604	69	0607	0110
AFT	SRD	0004		0607	31	0004	0569
	RAU	8002		0569	60	8002	1077
	MPY	CHI		1077	19	0985	0706
	SRD	0005		0706	31	0005	0571
	ALO	SPOT		0571	15	0975	0729
	ALO	TEMP		0729	15	0519	1023
	STL	SIGSC		1023	20	1127	0780
	ALO	SIGAB		0780	15	0639	0643
	RAU	8002		0643	60	8002	1101
	STU	THSIG		1101	21	0756	0509
	MPY	NTH		0509	19	0429	0550
	SRD	0006		0550	31	0006	0567
	STL	SIGTH	LOOP	0567	20	0427	0330
NR	LDD	AFTNR	0150	0418	69	0621	0150
AFTNR	RAL	8001		0621	65	8001	0779
	SRD	0005		0779	31	0005	0693
	RAU	8002		0693	60	8002	1151
	NZU	NON	NR	1151	44	0705	0418
NON	LDD	POSTL	0214	0705	69	0558	0214
POSTL	RAU	8003		0558	60	8003	1365
	MPY	LAMBD		1365	19	0415	0536
	SRD	0006		0536	31	0006	0453
	STL	D12		0453	20	0657	0410
	RAU	COLLB		0410	60	0326	0431
	NZU	CAL2	ZERO	0431	44	1435	0586
ZERO	RAM	D12		0586	67	0657	0611
	RAU	8002		0611	60	8002	0619
	MPY	COSA1		0619	19	0369	0490
	SRD	0007		0490	31	0007	0559

	ALO	R0004		0559	15	0354	0609
	STL	ZEE		0609	20	0563	0466
	RAM	D12		0466	67	0657	0661
	RAU	8002		0661	60	8002	0669
	MPY	SINA1		0669	19	0319	0540
	SLT	0004		0540	35	0004	1201
	SLO	8002		1201	16	8002	0659
	MPY	COSB1		0659	19	0421	0742
	AUP	R0002		0742	10	0352	0707
	STU	X		0707	21	0412	1415
	RAM	D12		1415	67	0657	0711
	RAU	8002		0711	60	8002	0719
	MPY	SINA1		0719	19	0319	0590
	SLT	0004		0590	35	0004	1251
	SLO	8002		1251	16	8002	0709
	MPY	SINC1		0709	19	0371	0792
	AUP	R0003		0792	10	0353	0757
	STU	Y		0757	21	0462	1465
OUTZ	RAU	ZEE	OUTZ	1465	60	0563	0617
ZOUT	BMI	POUT	ZOUT	0617	46	0420	0671
	RAM	ZEE		0671	67	0563	0667
	SLO	ZMAX		0667	16	0470	1025
POUT	BMI	XOUT	POUT	1025	46	0578	0420
	RAU	NINE		0420	60	1073	1177
	AUP	COLTH		1177	10	0350	0755
	STU	P0008		0755	21	0384	0787
	RAU	COLLB		0787	60	0326	0481
	STU	P0005		0481	21	0381	0534
	LDD	COLHY		0534	69	0434	0837
	STD	P0006		0837	24	0382	1485
	LDD	COLOX		1485	69	0342	0695
	STD	P0007		0695	24	0383	0636
	RAU	WS		0636	60	0315	0769
	STU	P0002		0769	21	0378	0531
	MPY	8003		0531	19	8003	0806
	STU	P0003		0806	21	0379	0432
	RAU	R0006		0432	60	0356	0761
	STU	P0001		0761	21	0377	0830
	LDD	SUMWI		0830	69	0334	0887
	STD	P0004		0887	24	0380	1183
XOUT	PCH	P0001	START	1183	71	0377	0300
	RAM	X		0578	67	0412	0717
	SLO	XMAX		0717	16	0520	1075
YOUT	BMI	YOUT	POUT	1075	46	0628	0420
	RAM	Y		0628	67	0462	0767
	SLO	YMAX		0767	16	0570	1125
THOR	BMI	THOR	POUT	1125	46	0678	0420
AFTER	LDD	AFTER	0150	0678	69	0581	0150
	STL	NR2		0581	20	1535	0638

	RAL	SIGTH		0638	65	0427	0631
	SLT	0006		0631	35	0006	0745
	DVR	SIG		0745	64	0341	0402
	SLT	0004		0402	35	0004	0613
	STL	FTH		0613	20	0817	0620
	SLO	NR2		0620	16	1535	0689
NOTH	BMI	NOTH	YESTH	0689	46	0842	0743
	RAL	SIGOX		0842	65	0795	0549
	SLT	0006		0549	35	0006	0663
	DVR	SIG		0663	64	0341	0452
	SLT	0004		0452	35	0004	0713
	STL	FOX		0713	20	0867	0670
	ALO	FTH		0670	15	0817	0721
	SLO	NR2		0721	16	1535	0739
NOOX	BMI	NOOX	YESOX	0739	46	0892	0793
	RAL	SIGHY		0892	65	0845	0599
	SLT	0006		0599	35	0006	0763
	DVR	SIG		0763	64	0341	0502
	SLT	0004		0502	35	0004	0813
	STL	FHY		0813	20	0917	0720
	ALO	FTH		0720	15	0817	0771
	ALO	FOX		0771	15	0867	0821
	SLO	NR2		0821	16	1535	0789
NOHY	BMI	NOHY	YESHY	0789	46	0942	0843
	RAU	FOUR		0942	60	0895	0649
	SLT	0005		0649	35	0005	0811
YESHY	STU	ID	COLL	0811	21	0516	0819
	RAU	THREE		0843	60	0304	0759
	SLT	0005		0759	35	0005	0871
	STU	ID		0871	21	0516	0869
	RAU	COLHY		0869	60	0434	0839
	AUP	ONED		0839	10	0403	0807
YESOX	STU	COLHY	COLL	0807	21	0434	0819
	RAU	TWO		0793	60	0454	0809
	SLT	0005		0809	35	0005	0921
	STU	ID		0921	21	0516	0919
	RAU	COLOX		0919	60	0342	0747
	AUP	ONED		0747	10	0403	0857
YESTH	STU	COLOX	COLL	0857	21	0342	0819
	RAU	ONEB		0743	60	0438	0893
	STU	ID		0893	21	0516	0969
	RAU	COLTH		0969	60	0350	0805
	AUP	ONED		0805	10	0403	0907
WATE	STU	COLTH	WATE	0907	21	0350	0503
	RAU	WS		0503	60	0315	1019
	MPY	SIGSC		1019	19	1127	0448
	DVR	THSIG		0448	64	0756	0566
COLL	STL	WS	COLL	0566	20	0315	0819
	RAU	COLLB		0819	60	0326	0681

	AUP	ONED		0681	10	0403	0957
	STU	COLLB		0957	21	0326	0829
	LDD	ID		0829	69	0516	1069
	TLU	1850		1069	84	1850	0855
VALU	ALO	VALU	8002	0855	15	0608	8002
ACT2	RAU	0000	ACT2	0608	60	0000	0905
	SLT	0005		0905	35	0005	0967
	SRT	0005		0967	30	0005	0879
	STU	MASS		0879	21	0584	0937
AFR	LDD	AFR	0150	0937	69	0640	0150
	STD	ENR		0640	24	0943	0396
	RAU	ONED		0396	60	0403	1007
	SRT	0002		1007	30	0002	0863
	AUP	MASS		0863	10	0584	0889
	STU	AONE		0889	21	0394	0797
	RAU	MASS		0797	60	0584	0939
	SLT	0002		0939	35	0002	0945
	SUP	ONED		0945	11	0403	1057
	SRT	0002		1057	30	0002	0913
	DVR	AONE		0913	64	0394	0654
	RAU	8002		0654	60	8002	0963
	MPY	8003		0963	19	8003	0688
	SRT	0004		0688	30	0004	0699
	STU	ALPHA		0699	21	0704	1107
	SLO	8002		1107	16	8002	1515
	RAU	ONE		1515	60	0347	1301
	SUP	ALPHA		1301	11	0704	0859
	MPY	ENR		0859	19	0943	0464
	SRD	0009		0464	31	0009	0987
	AUP	ONEE		0987	10	0440	0995
	SUP	8002		0995	11	8002	0553
	SLO	8002		0553	16	8002	0861
	MPY	ETWO		0861	19	0361	0482
	STD	EONE		0482	24	1585	0738
	SRD	0007		0738	31	0007	1157
	STL	ETWO		1157	20	0361	0514
	SLO	EMIN		0514	16	1017	0971
	BMI	LOW	ESCAT	0971	46	0574	1175
LOW	RAU	R0006		0574	60	0356	0911
	STU	P0001		0911	21	0377	0880
	RAU	COLLB		0880	60	0326	0731
	STU	P0005		0731	21	0381	0634
	LDD	COLHY		0634	69	0434	1037
	STD	P0006		1037	24	0382	1685
	LDD	COLOX		1685	69	0342	1045
	STD	P0007		1045	24	0383	0686
	RAU	ONE		0686	60	0347	1351
	AUP	COLTH		1351	10	0350	0955
	STU	P0008		0955	21	0384	1087

	RAU	WS		1087	60	0315	1119
	STU	P0002		1119	21	0378	0781
	MPY	8003		0781	19	8003	0856
	STU	P0003		0856	21	0379	0532
	LDD	SUMWI		0532	69	0334	1137
	STD	P0004		1137	24	0380	1233
	PCH	P0001	START	1233	71	0377	0300
ESCAT	RAU	ETWO		1175	60	0361	1565
	SRT	0002		1565	30	0002	1021
	DVR	EONE		1021	64	1585	0446
	LDD	NXT	0110	0446	69	0749	0110
NXT	SRD	0005		0749	31	0005	1013
	STL	AID		1013	20	1067	0770
	RAL	ALPHA		0770	65	0704	0909
	SLT	0004		0909	35	0004	1169
	LDD	AUX	0110	1169	69	0572	0110
AUX	SRD	0002		0572	31	0002	0831
	DVR	AID		0831	64	1067	0728
	AUP	AID		0728	10	1067	1071
	SUP	8002		1071	11	8002	0929
	SLO	8002		0929	16	8002	1187
	MPY	AONE		1187	19	0394	0564
	RAU	8002		0564	60	8002	1123
	MPY	FIVE		1123	19	0346	0616
	SRD	0005		0616	31	0005	0881
	STL	COSAP		0881	20	1885	0788
	RAU	8002		0788	60	8002	0847
	MPY	8003		0847	19	8003	0622
	SLT	0001		0622	35	0001	0979
	STU	AID		0979	21	1067	0820
	RAU	ONED		0820	60	0403	1207
	SRT	0003		1207	30	0003	1865
	SLO	AID		1865	16	1067	1121
	SLT	0001		1121	35	0001	1227
	NZU	NON2	NX	1227	44	0931	0582
NX	LDD	SQ	0110	0582	69	1985	0110
SQ	SRD	0001		1985	31	0001	0491
	STL	SINAP	AZMTH	0491	20	1095	0498
NON2	SRD	0001		0931	31	0001	1237
	STL	SINAP	AZMTH	1237	20	1095	0498
AZMTH	LDD	NXNR	0150	0498	69	1401	0150
NXNR	RAU	8002		1401	60	8002	0959
	MPY	TPI		0959	19	0512	0632
	SLT	0005		0632	35	0005	1145
	STU	AID		1145	21	1067	0870
	SLO	8002		0870	16	8002	1029
	LDD	AFPHI	0000	1029	69	0682	0000
AFPHI	STL	SINBP		0682	20	1287	0690
	RAU	AID		0690	60	1067	1171

AFCOS CAL2	LDD	AFCOS	0049	1171	69	0624	0049
	STL	COSBP	MEANF	0624	20	1079	0374
	RAU	SINAP		1435	60	1095	0799
	MPY	COSBP		0799	19	1079	0600
	SRT	0002		0600	30	0002	1257
	STU	XPOND		1257	21	0562	0666
	RAU	SINAP		0666	60	1095	0849
	MPY	SINBP		0849	19	1287	0658
	SRT	0002		0658	30	0002	0716
	STU	YPOND		0716	21	0920	1173
	RAU	COSAP		1173	60	1885	0989
	SRT	0003		0989	30	0003	0897
	STU	ZPOND		0897	21	0552	1005
	RAU	YPOND		1005	60	0920	1225
	MPY	SINCI		1225	19	0371	0992
	SLT	0001		0992	35	0001	0899
	STU	AID		0899	21	1067	0970
	RAU	XPOND		0970	60	0562	1117
	MPY	COSA1		1117	19	0369	0740
	SLT	0001		0740	35	0001	0947
	STU	STORE		0947	21	0602	1055
	RAU	ZPOND		1055	60	0552	1307
	MPY	SINA1		1307	19	0319	0790
	SLT	0001		0790	35	0001	0997
	AUP	STORE		0997	10	0602	1357
	STU	STORE		1357	21	0602	1105
	SLO	8002		1105	16	8002	1063
	MPY	COSB1		1063	19	0421	1042
	SLT	0001		1042	35	0001	0949
	SUP	AID		0949	11	1067	1221
	STU	DELXD		1221	21	0576	1129
	RAU	YPOND		1129	60	0920	1275
	MPY	COSB1		1275	19	0421	1092
	SLT	0001		1092	35	0001	0999
	STU	AID		0999	21	1067	1020
	RAU	STORE		1020	60	0602	1407
	MPY	SINCI		1407	19	0371	1142
	SLT	0001		1142	35	0001	1049
	AUP	AID		1049	10	1067	1271
STU	DELYD		1271	21	0626	1179	
RAU	XPOND		1179	60	0562	1167	
MPY	SINA1		1167	19	0319	0840	
SLT	0001		0840	35	0001	1047	
STU	AID		1047	21	1067	1070	
RAU	ZPOND		1070	60	0552	1457	
MPY	COSA1		1457	19	0369	0890	
SLT	0001		0890	35	0001	1097	
SUP	AID		1097	11	1067	1321	
SLT	0003		1321	35	0003	1229	

	STU	COSA1		1229	21	0369	0672
	RAU	DELXD		0672	60	0576	0981
	MPY	8003		0981	19	8003	0906
	SLT	0006		0906	35	0006	1371
	STU	AID		1371	21	1067	1120
	RAU	DELYD		1120	60	0626	1031
	MPY	8003		1031	19	8003	0956
	SLT	0006		0956	35	0006	1421
	AUP	AID		1421	10	1067	1471
	RAL	8003		1471	65	8003	1279
	LDD	B	0110	1279	69	0732	0110
B	STL	SINA1		0732	20	0319	0722
	RAU	DELXD		0722	60	0576	1081
	SRT	0001		1081	30	0001	1337
	DVR	SINA1		1337	64	0319	0930
	SLT	0002		0930	35	0002	1387
	STL	COSB1		1387	20	0421	0674
	RAU	DELYD		0674	60	0626	1131
	DVR	SINA1		1131	64	0319	0980
	SLT	0002		0980	35	0002	1437
	STL	SINC1		1437	20	0371	0724
	RAM	D12		0724	67	0657	0961
	STL	D12		0961	20	0657	0460
	RAU	8002		0460	60	8002	1219
	MPY	COSA1		1219	19	0369	0940
	SLT	0003		0940	35	0003	1099
	AUP	ZEE		1099	10	0563	1217
	STU	ZEE		1217	21	0563	0766
	BMI	POUT	ZIN	0766	46	0420	1170
ZIN	RAU	DELXD		1170	60	0576	1181
	MPY	D12		1181	19	0657	0778
	SRD	0004		0778	31	0004	0541
	ALO	X		0541	15	0412	1267
	STL	X		1267	20	0412	0816
	RAM	X		0816	67	0412	1317
	SLO	XMAX		1317	16	0520	1325
	BMI	XIN	POUT	1325	46	0828	0420
XIN	RAU	DELYD		0828	60	0626	1231
	MPY	D12		1231	19	0657	0878
	SRD	0004		0878	31	0004	0591
	ALO	Y		0591	15	0462	1367
	STL	Y		1367	20	0462	0866
	RAM	Y		0866	67	0462	1417
	SLO	YMAX		1417	16	0570	1375
	BMI	THOR	POUT	1375	46	0678	0420
NTH	00	0006	2500	0429	00	0006	2500
SINOH	00	0001	5276	0433	00	0001	5276
NINTN	00	0000	1900	0368	00	0000	1900
SIG1	00	0000	1150	0336	00	0000	1150

TWO8	00	0000	2800	0518	00	0000	2800
FIVE2	00	0000	5200	0568	00	0000	5200
SIG2	00	0000	1180	0436	00	0000	1180
SIX4	00	0000	6400	0618	00	0000	6400
SEV6	00	0000	7600	0668	00	0000	7600
TEN5	00	0001	0500	0718	00	0001	0500
ONE11	00	0111	3000	0768	00	0111	3000
ELEV8	00	0001	1800	0818	00	0001	1800
ONE25	00	0001	2500	0868	00	0001	2500
ONE40	00	0001	4000	0918	00	0001	4000
ONE85	00	0001	8550	0968	00	0001	8550
ONE32	00	1320	0000	0486	00	1320	0000
THRE3	03	3780	0000	0340	03	3780	0000
TWO27	00	0000	2270	0468	00	0000	2270
SIXTY	60	0000	0000	0650	60	0000	0000
ONE	00	0100	0000	0347	00	0100	0000
ONEB	00	0010	0000	0438	00	0010	0000
FIVE	50	0000	0000	0346	50	0000	0000
ONEC	00	0001	0000	0392	00	0001	0000
DEL1	00	0000	0010	0561	00	0000	0010
DEL2	00	0000	0020	0312	00	0000	0020
SPLIT	00	2000	0000	0500	00	2000	0000
ZMAX	00	3700	0000	0470	00	3700	0000
XMAX	00	3650	0000	0520	00	3650	0000
YMAX	00	3650	0000	0570	00	3650	0000
NINE	00	9000	0000	1073	00	9000	0000
SIGOX	00	0000	1554	0795	00	0000	1554
SIGHY	00	0001	3439	0845	00	0001	3439
SIGNI	00	0000	0228	0700	00	0000	0228
EMIN	00	0000	1000	1017	00	0000	1000
TPI	00	0006	2832	0512	00	0006	2832
FOUR	00	0000	0004	0895	00	0000	0004
ONEE	00	1000	0000	0440	00	1000	0000
THREB	00	0000	0300	0404	00	0000	0300
TWO	00	0000	0002	0454	00	0000	0002
THREE	00	0000	0003	0304	00	0000	0003
ONED	00	0000	0100	0403	00	0000	0100
FIVEB	00	0005	0000	0320	00	0005	0000
ZEROP	00	0000	00 0	317	00	0000	0000
SPOT	00	0000	1050	0975	00	0000	1050
				470	00	3300	0000
				520	00	3100	0000
				570	00	3100	0000
				429	00	0015	3813
				795	00	0000	1577
				845	00	0000	9312
				700	00	0000	0560
				433	00	0001	1449

TABLE LOOKUP FOR PEAK PARAMETERS

The data for each peak is given by a group of six words. The last 5 digits of each gives the particular parameter value.

<u>Position</u>	<u>Argument</u>	<u>Function</u>
1900	00010	02184
1901	00011	00190
1902	00012	06871
1903	00013	00445
1904	00014	05555
1905	00015	01468
1906	00020	02348
1907	00021	00170
1908	00022	09340
1909	00023	00957
1910	00024	04651
1911	00025	01106
1912	00030	05955
1913	00031	00440
1914	00032	06235
1915	00033	01365
1916	00034	07692
1917	00035	07668
1918	00040	06920
1919	00041	00150
1920	00042	09380
1921	00043	08500
1922	00044	02439
1923	00045	00896
1924	00050	11315
1925	00051	00300
1926	00052	03780
1927	00053	00989
1928	00054	03774
1929	00055	03506
1930	00060	12100
1931	00061	00280
1932	00062	04610
1933	00063	02079
1934	00064	03333
1935	00065	02926
1936	00070	12940

1937	00071	00380
1938	00072	01318
1939	00073	00100
1940	00074	04545
1941	00075	05818
1942	00080	17080
1943	00081	00190
1944	00082	03770
1945	00083	04560
1946	00084	01887
1947	00085	01324

TABLE LOOKUP FOR $\Psi(x,t)$ AND $\chi(x,t)$

For a given 10 digit word, digits 4 through 7 carry the value of $\Psi(x,t)$ and digits 8 through 10 carry the corresponding value of $\chi(x,t)$. The values are 0-4 and 0-3 numbers respectively. The first digit gives the peak number

1700	10100	35058
1701	10200	40061
1702	10300	46065
1703	10400	55074
1704	10500	67079
1705	10600	84084
1706	10701	10091
1707	10801	50099
1708	10902	11110
1709	11003	03125
1710	11104	39141
1711	11206	30151
1712	11308	82153
1713	11411	95157
1714	11515	51147
1715	11619	22138
1716	11722	63125
1717	11825	27068
1718	11926	71042
1719	20100	50069
1720	20200	59074
1721	20300	72081
1722	20400	90087
1723	20501	17097

1724	20601	59109
1725	20702	27119
1726	20803	35132
1727	20905	02158
1728	21007	46171
1729	21110	79176
1730	21214	94180
1731	21319	59163
1732	21424	14137
1733	21527	82088
1734	21629	88030
1735	30100	06025
1736	30200	07026
1737	30300	08027
1738	30400	09029
1739	30500	11031
1740	30600	14034
1741	30700	18036
1742	30800	24041
1743	30900	34045
1744	31000	50050
1745	31100	74055
1746	31201	14061
1747	31301	70071
1750	31402	50077
1751	31503	55078
1752	31604	88078
1753	31706	43076
1754	31808	12074
1755	31909	80069
1756	32011	31057
1757	32112	44040
1758	32213	04017
1759	40100	56074
1760	40200	67079
1761	40300	82087
1762	40401	03095
1763	40501	36106
1764	40601	88119
1765	40702	75135
1766	40804	17152
1767	40906	41180
1768	41009	72189
1769	41114	19205
1770	41219	54280
1771	41325	07144
1772	41429	72069
1773	41532	41032
1774	50100	14036

1775	50200	17040
1776	50300	21044
1777	50400	26049
1778	50500	36052
1779	50600	54060
1780	50700	88072
1781	50801	51080
1782	50902	62103
1783	51004	40110
1784	51106	97106
1785	51210	19117
1786	51313	65087
1787	51416	63071
1788	51518	37024
1789	60100	16039
1790	60200	19043
1791	60300	24047
1792	60400	32052
1793	60500	45060
1794	60600	69070
1795	60701	18082
1796	60802	11097
1797	60903	76116
1800	61006	36132
1801	61109	91123
1802	61213	96118
1803	61317	63109
1804	61419	82042
1805	70100	09029
1806	70200	10032
1807	70300	12036
1808	70400	14038
1809	70500	17042
1810	70600	23048
1811	70700	32058
1812	70800	47072
1813	70900	73090
1814	71001	15121
1815	71101	82158
1816	71202	80200
1817	71304	17249
1818	71405	92238
1819	71507	99305
1820	71610	19311
1821	71712	25290
1822	71813	87176
1823	71914	76006
1824	80100	34057
1825	80200	39060

1826	80300	45065
1827	80400	53070
1828	80500	63075
1829	80600	79082
1830	80701	01090
1831	80801	35097
1832	80901	89110
1833	81002	72123
1834	81103	98138
1835	81205	82147
1836	81308	34163
1837	81411	57179
1838	81515	36151
1839	81619	40132
1840	81723	21123
1841	81826	20087
1842	81927	84016
1600	24160	31606
1606	16800	21665
1665	24166	81621
1621	19162	41660
1660	10166	31620
1620	31000	81641
1641	16800	21649
1649	24160	21605

TABLE LOOKUP FOR ATOMIC MASSES

The mass is given by the last five digits.

1850	00001	00232
1851	00002	00016
1852	00003	00001
1853	00004	00014

SUBROUTINE exp{-x}

<u>Position</u>	<u>Oper-</u> <u>ation</u>	<u>Data</u> <u>Address</u>	<u>Instruction</u> <u>Address</u>
1605	30	0001	1662
1662	11	8003	1669
1669	35	0001	1626
1626	15	8001	1631
1631	35	0004	1642
1642	10	1645	1650
1650	11	8003	1608
1608	24	1661	1664
1664	18	1668	1623
1623	45	1676	1679
1676	46	1629	1630
1630	69	1633	1637
1629	69	1632	1637
1679	69	1634	1637
1637	22	1643	1647
1647	60	1602	1607
1607	11	1663	1667
1667	30	0001	1674
1674	16	8002	1635
1635	19	8003	1658
1619	89	1250	9381
1658	24	1673	1627
1627	65	8003	1636
1636	31	0002	1646
1646	15	1601	1655
1655	10	1609	1666
1666	16	8002	1625
1625	30	0001	1638
1638	64	8001	1644
1644	16	1648	1653
1653	35	0001	1659
1659	10	8002	1670
1670	15	1673	1677
1677	11	8001	1639
1639	16	8002	1651
1651	30	0001	1657
1657	64	8001	1652

<u>Position</u>	<u>Oper-</u> <u>ation</u>	<u>Data</u> <u>Address</u>	<u>Instruction</u> <u>Address</u>	
1652	60	8002	1661	
1661	19	0000	1671	
1671	31	0009	1643	
1643	00	0000	1603	
1624	43	4294	4819	
1663	50	0000	0000	
1645	19	1610	1671	
1633	35	0000	1603	SUBROUTINE
1632	31	0000	1603	
1634	00	0000	1603	exp {-x}
1601	11	3167	0182	(continued)
1609	49	1478	1154	
1648	52	1153	3783	
1610	11	2201	8454	
1611	14	1253	7545	
1612	17	7827	9410	
1613	22	3872	1139	
1614	28	1838	2931	
1615	35	4813	3892	
1616	44	6683	5922	
1617	56	2341	3252	
1618	70	7945	7844	
1619	89	1250	9381	

SUBROUTINE FOR SINE AND COSINE

49	24	0003	0006
6	10	0009	0013
13	46	0025	0017
17	11	0020	0025
	24	0003	0025
25	46	0028	0029
28	10	0032	0037
29	11	0032	0037
37	21	0042	0045
45	46	0048	0099
48	10	0002	0007
99	11	0002	0007

7	21	0012	0015
15	46	0018	0019
18	10	0022	0027
19	11	0022	0027
27	21	0082	0035
35	68	8003	0043
43	15	0046	0001
1	35	0001	0057
57	20	0011	0014
14	60	8001	0021
21	19	8001	0005
5	21	0056	0059
59	60	0012	0069
69	46	0072	0073
72	60	0082	0087
87	46	0092	0050
73	60	0082	0038
38	46	0050	0092
92	61	0095	0051
51	19	0056	0030
30	10	0091	0096
96	61	8003	0053
53	19	0056	0041
41	10	0089	0094
94	61	8003	0052
52	19	0056	0044
44	10	0085	0090
90	61	8003	0098
98	19	0056	0054
54	10	0034	0040
40	61	8003	0047
47	19	0056	0055
55	10	0093	0097
97	60	8003	0008
8	19	0011	0031
31	21	0036	0039
39	65	0042	0004
4	46	0070	0071
70	65	0036	0003
71	66	0036	0003
50	61	0056	0064
64	24	0079	0033
33	19	0086	0058
58	10	0063	0068
68	61	8003	0026
26	19	0079	0074
74	10	0062	0067
67	61	8003	0076
76	19	0079	0078

78	10	0061	0016
16	61	8003	0075
75	19	0079	0088
88	10	0010	0066
66	61	8003	0024
24	19	0079	0080
80	10	0060	0065
65	61	8003	0023
23	19	0079	0083
83	10	0093	0031
9	15	7079	6327
20	62	8318	5307
32	31	4159	2654
2	15	7079	6327
22	07	8539	8163
46	07	8539	8163
95	00	0000	0025
91	00	0000	2756
89	00	0019	8413
85	00	0833	3333
34	01	6666	6667
93	10	0000	0000
86	00	0000	0002
63	00	0000	0276
62	00	0002	4802
61	00	0138	8889
10	00	4166	6667
60	05	0000	0000

SUBROUTINE FOR RANDOM NUMBER

110	45	0114	8001
114	24	0118	0121
121	20	0127	0106
106	65	0109	0113
113	10	8001	0122
122	19	0127	0115
115	65	8003	0124

124	10	0127	0131
131	16	8002	0139
139	64	8001	0130
130	16	8001	0138
138	46	0100	0108
100	15	8001	0107
107	15	8001	0116
116	10	0119	0123
123	30	0001	0129
129	16	8002	0137
137	19	8001	0124
108	15	8001	0118
109	50	0000	0000
119	00	0000	0050
156	60	0159	0163
150	24	0153	0156
163	19	0166	0160
160	20	0166	0169
169	21	0174	0177
177	60	0180	0151
151	19	0154	0152
152	15	0174	0179
179	20	0154	0153
159	11	6226	1467
180	11	6226	1467
154	01	3508	5171
166	76	7299	2089

SUBROUTINE FOR NATURAL LOG

224	24	0227	0280
280	69	0231	0285
285	24	0288	0291
214	24	0227	0221
221	69	0232	0285
291	46	0299	0295
295	45	0298	0299
299	01	9999	9999

298	36	0000	0223
223	20	0277	0281
281	65	8003	0230
230	15	0233	0238
238	31	0001	0245
245	20	0249	0202
202	35	0001	0209
209	16	0212	0217
217	16	8001	0225
225	35	0209	0246
246	64	0249	0239
239	20	0244	0247
247	60	8001	0206
206	19	8001	0237
237	31	0000	0215
231	10	0000	0000
232	23	0258	5093
215	20	0222	0228
228	60	8001	0235
235	19	0240	0236
236	10	0243	0201
201	60	8003	0216
216	19	0222	0200
200	10	0203	0210
210	60	8003	0218
218	19	0222	0204
204	10	0207	0211
211	60	8003	0219
219	19	0222	0226
226	10	0229	0234
234	60	8003	0241
241	19	0244	0205
205	10	0208	0213
213	30	0001	0220
220	15	8001	0278
229	86	8591	7180
207	28	9335	5240
203	17	7522	0710
243	09	4376	4760
240	19	1337	7140
212	31	6227	7660
233	31	6227	7660
208	50	0000	0000
278	21	0282	0286
286	61	0277	0283
283	10	0287	0292
287	00	0000	0004
292	30	0001	0279
279	60	8002	0242

242	10	0282	0289
289	19	0288	0227

DATA EXTRACTION PROGRAM

After reading the output cards into this program locations 277, 278, 281, 282, 283, 284, 285, 286, 287, 288, 289, and 290 will contain the necessary results.

405	00	0100	0000
60	70	0251	0065
65	60	0331	0070
70	10	0405	0075
75	21	0331	0080
80	60	0258	0085
85	44	0410	0090
90	60	0251	0092
92	31	0003	0095
95	10	0277	0100
100	21	0277	0105
105	60	0252	0107
107	31	0003	0110
110	10	0278	0115
115	21	0278	0120
120	60	0281	0125
125	10	0255	0130
130	21	0281	0135
135	60	0282	0140
140	10	0256	0145
145	21	0282	0150
150	60	0283	0155
155	10	0257	0160
160	21	0283	0060
410	60	0251	0412
412	31	0003	0415
415	10	0284	0420
420	21	0284	0425
425	60	0252	0428
428	31	0003	0430
430	10	0285	0435
435	21	0285	0440
440	60	0286	0445

445	10	0255	0450
450	21	0286	0455
455	60	0287	0460
460	10	0256	0465
465	21	0287	0470
470	60	0288	0475
475	10	0257	0480
480	21	0288	0485
485	60	0289	0490
490	10	0258	0495
495	21	0289	0060
80	60	0258	0083
83	35	0005	0085
85	30	0005	0087
87	21	0050	0088
88	44	0410	0090
490	10	0050	0495
495	21	0289	0500
500	60	0253	0505
160	21	0283	0360
360	60	0253	0500
505	21	0290	0060
505	30	0003	0510
510	10	0290	0515
515	21	0290	0060

ABSTRACT

We have undertaken to develop a method for determining the resonance escape probability of homogeneous reactors containing aqueous solutions of a resonance absorber. $\text{Th}(\text{NO}_3)_4$ was selected as a salt since it is readily dissolvable in water. Even at the highest concentration, the atomic densities of thorium and nitrogen are small compared to hydrogen and oxygen. Only the latter two contribute significantly to the slowing down in the high energy range; therefore, a water Monte Carlo serves adequately as the neutron supply to the resonance region of thorium.

In order to find an escape probability we determine the ratio of the number of neutrons that attain energies below the resonance region to the number that appear in the resonance region for the first time. The difference between the two numbers in the ratio occurs due to absorption by the resonance absorber, in this case thorium, and due to leakage.

The initial source of neutrons comes from $\text{H}^2(d,n)\text{He}^3$ reaction where the deuteron beam strikes the deuterium target at the center of one face of the containing parallelepiped.

Once the water Monte Carlo is run one has a set of data cards which can be used as the input data to a second Monte Carlo designed to calculate the resonance escape probability. Our prime concern is this second Monte Carlo.

The resonance escape Monte Carlo is a direct analog type using known physical distributions and laws. The decisions about what events occur in the history of a neutron are based on these distributions and laws. The detailed effect of the thorium resonances on the number of neutrons absorbed is described by the cross section as a function of energy. A Breit-Wigner Doppler broadened single level formulation gives the scattering and absorption parts of the cross section as a function of energy. Given a neutron-thorium interaction, the neutron is either absorbed or scattered with probabilities $\frac{\sigma_{ab}}{\sigma_{ab} + \sigma_{sc}}$ and $\frac{\sigma_{sc}}{\sigma_{ab} + \sigma_{sc}}$. A new statistical weight is assigned the neutron by taking the latter fraction of the old weight. A new neutron is picked from the source supply only after the previous neutron has delivered a weight to low energy or to the exterior of the pile.

The heart of the Monte Carlo method lies in the determination of a random variable, distributed according to some known probability function. This requires a source of

random numbers which in our case is provided by the IBM-650 computer.

The resonance escape probability as a function of thorium number density fits very closely to a straight line with small negative slope throughout the whole range of stable concentrations. The Monte Carlo statistics provides probable errors of less than 0.3% for all five points calculated. Each of the five points lies close enough to the straight line of least squares fit to give an error less than 0.3%.

A theoretical determination of the resonance escape probability based on resonance integral theory for the eight peaks used in the Monte Carlo calculation gives good enough agreement to make both methods plausible.

Although other resonance escape calculations have been done by the Monte Carlo method, they have been for radically different systems. In all such cases the system was heterogeneous with "lumped" uranium for the absorber. Therefore comparisons between existing Monte Carlo calculations is impossible. We hope to be able to provide experimental verification for the applicability of the Monte Carlo model.